NAL TR-9T

UDC 533.6.011.35
: 517.93

THCHNICAL REPORT OF NATIONAL AERONAUTICAL LABORATORY

TR-9T

Studies on the Small Disturbance Theory of Transonic Flow (I)

—Nonlinear Correction Theory—

Iwao HOSOKAWA

July 1962

NATIONAL AERONAUTICAL LABORATORY

MITAKA, TOKYO, JAPAN

Studies on the Small Disturbance Theory of Transonic Flow (I)

—Nonlinear Correction Theory—

By Iwao HOSOKAWA*

CONTENTS

Foreword

This report consists of three papers, which deal with a new approach to the small disturbance theory of transonic flow (the transonic approximation). The basic idea of the method and its formulation are given in the first paper: based on the view point that it is the quadratic nonlinearity of the basic equation which is essential to the characteristic feature of transonic flow, such as shock waves, the nonlinear correction term of the velocity field is estimated in as general a manner as possible in order to complement the solution of the linearized transonic flow theory recently proposed by Oswatitsch and Maeder. To use the linearized theory as a starting point is advantageous for the formalism of solutions. Here it is worthwhile to note that recently Maeder and Thommen** derived almost the same method as the author's, by dealing with the integral equation transformed from the original basic equation (through Green's theorem). The other papers illustrate interesting examples of application of the method: about the flows on a sinusoidal wall and on a symmetric circular-arc aerofoil. We shall then grasp a physical image of the continuous transition of the transonic flow with increasing Mach number from subsonic to supersonic in a reasonable manner.

* The First Aerodynamics Division

** P. F. Maeder and H. G. Thommen: Linearized Transonic Flow About Slender Bodies at Zero Angle of Attack, Transact. ASME, J. Appl. Mech., 481-490 (Dec. 1961)

A Refinement of the Linearized Transonic Flow Theory*

A new method is proposed to calculate the velocity and pressure distributions around a thin symmetrical aerofoil or a slender body of revolution flying at transonic speed. It is essentially a refinement of the linearized transonic flow theory due to Oswatitsch and Maeder, such that a correction term is introduced to take account of the nonlinear character of the transonic flow. As examples of application, a symmetrical circular-arc aerofoil and a circular-arc body of revolution in the sonic flow are dealt with, and the results are found to be in good agreement with experiments, except for the rear portion in the latter case.

§ 1. Introduction

As is well known, the flow around an obstacle in the nearly sonic free stream is governed by a nonlinear differential equation of mixed type. As a practical approximation method, the method of integral equation has been contrived by Oswaititsch and developed by Gullstrand and Spreiter[1),2)]. But the method is only applicable to flows with free stream Mach number near critical, though it can account for the appearance of normal shock waves.

Oswatitsch[3)] and Maeder[4)] tried linearization of the transonic flow theory. Although this method seems to be very powerful, it has two unsatisfactory points; first the calculated flow is not influenced by the mixed-flow character that makes the essence of the transonic flow as Miles[5)] has pointed out before, and secondly, according to Maeder's method of determining the value of the assumed constant K (see (2.2)), the movement of the sonic point on the aerofoil with increasing Mach number seems to be incorrectly given at least for a circular-arc aerofoil, as is seen in Fig. 1.

In this paper, a refinement of the method is proposed to remove such defects and take account of the mixed-flow and nonlinear characters, by approximately calculating a correction term to the linearized transonic flow theory.

Recently, Spreiter[6),7)] has put forward another simple and powerful method, called local linearization method. Our present method seems to given results which are comparable with those given by Speriter's method (see Fig. 2 and 3), but ours is different from his in accounting for the occurrence of the transonic normal shock waves on the obstacle.

§ 2. Basic Equation

The basic equation for the transonic flow can be written in the form:

$$(1-M_\infty^2)\Phi_{xx}+\Phi_{yy}+\Phi_{zz}=(\gamma+1)M_\infty^2\Phi_x\Phi_{xx} \tag{2.1}$$

where $U_\infty\Phi$ is the perturbation velocity potential, U_∞ and M_∞ are the free stream velocity and Mach number respectively, γ is the ratio of specific heats, and the x-axis is taken in the direction of the free stream. Maeder has approximated (2.1) by a linear equation:

$$(1-M_\infty^2)\varphi_{xx}+\varphi_{yy}+\varphi_{zz}=K\varphi_x \tag{2.2}$$

where K is a certain constant to be determined appropriately. This can be integrated subject to the usual linear boundary condition, thus giving a finite continuous solution

$$\varphi=\varphi(x, y, z;\ K) \tag{2.3}$$

for each M_∞.

Let us introduce a correction potential g defined as

$$\Phi=\varphi+g \tag{2.4}$$

* Journal of the Physical Society of Japan, Vol. 15, No. 1, P. 149~157, January, 1960.

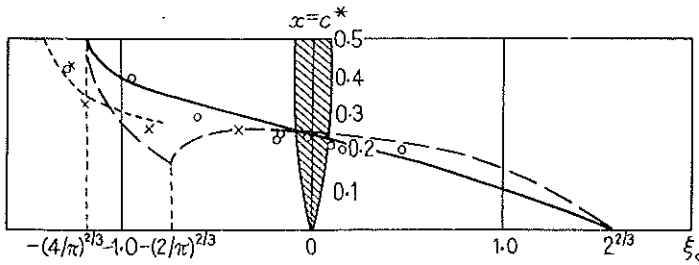

Fig. 1. Sonic point behaviour on the symmetrical circular-arc aerofoil with ξ_∞.

Then we have, by (2.1)–(2.4),

$$g_{yy}+g_{zz}=\frac{\partial}{\partial x}\left[\{(M_\infty^2-1)+(\gamma+1)M_\infty^2\varphi_x\}g_x+\frac{1}{2}(\gamma+1)M_\infty g_x^2\right]+\{(\gamma+1)M_\infty^2\varphi_{xx}-K\}\varphi_x\,. \tag{2.5}$$

The left-hand side of the equation is reduced to g_{yy} in the two-dimensional case, while it may be expressed as $g_{rr}+(1/r)g_r$ in the axisymmetric case where $r=(y^2+z^2)^{1/2}$. Also (2.5) shows the mixed-flow character such that it changes type according as

$$(M_\infty^2-1)+(\gamma+1)M_\infty^2\Phi_x\gtreqless 0 \tag{2.6}$$

as should be expected. Here the equality holds for the sonic line or surface.

Now as a first step to find the solution g of (2.5) valid in the neighbourhood of the obstacle, let us consider the order of magnitude of various quatities in (2.5). According to Guderley[8], the both sides of (2.1) are considered to be of the same order $O(\tau^2)$. Here τ is defined as an expansion parameter such that

$$\Phi=O(\tau), \qquad (\gamma+1)M_\infty^2\tau/(1-M_\infty^2)=O(1) \tag{2.7}$$

and

$$x=L\bar{x}, \qquad y=L\tau^{1/2}\bar{y}, \qquad z=L\tau^{1/2}\bar{z} \tag{2.8}$$

where L is the length of the thin or slender obstacle, $\bar{x}$, $\bar{y}$ and $\bar{z}$ being $O(1)$. If t is the thickness ratio, it is related to τ as

$$\tau=O(t^{2/3}) \qquad \text{or} \qquad \tau=O(t^2) \tag{2.9}$$

in the two-dimensional or axisymmetric case respectively.

Then the boundary condition of g on the obstacle will be that $g_y=O(\tau^{5/2})$, $g_z=O(\tau^{5/2})$ there, provided that φ has already been determined so as to satisfy the usual linear boundary condition. That is, if $U_\infty\Phi_x=u$ and $U_\infty\Phi_y=v$,

$$\frac{\Phi_y}{1+\Phi_x}\cong\varphi_x+g_x, \qquad \frac{v}{U_\infty+u}=\frac{v}{U_\infty}-\frac{v}{U_\infty}\frac{u}{U_\infty}+\cdots$$

$$\varphi_y=\frac{v}{U_\infty}$$

and hence, with the aid of (2.7) and (2.8) we have

$$\left.\begin{aligned} &g_y=O\left(\frac{v}{U_\infty}\frac{u}{U_\infty}\right)=O(\tau^{3/2}\tau)=O(\tau^{5/2})\\ &\text{and similarly}\\ &g_z=O(\tau^{5/2}) \end{aligned}\right\} \tag{2.10}$$

except near the nose and tail of the obstacle. Therefore it is concluded that

$$g_{yy}+g_{zz}=O(\tau^3) \tag{2.11}$$

in the neighbourhood of the obstacle, while the right-hand side of (2.5) is generally considered

as $O(\tau^2)$. Thus we may consider the left-hand side of (2.5) to be negligible in comparison with the right-hand side, at least near the obstacle. (For the axisymmetric case the estimation of order of magnitude should be performed in a slightly different manner. But the conclusion is the same as for the two-dimensional case.)

Now the basic equation can be simplified in the form:

$$\frac{\partial}{\partial x}\left[\{(M_\infty^2-1)+(\gamma+1)M_\infty^2\varphi_x\}g_x+\frac{1}{2}(\gamma+1)M_\infty g_x^2\right]+\{(\gamma+1)M_\infty^2\varphi_{xx}-K\}\varphi_x=0. \tag{2.12}$$

Further g is subjected to the condition, that it should vanish when the last inhomogeneous term in (2.5) or (2.12) vanishes identically. That is,

$$g\equiv 0, \qquad \text{when} \quad \{(\gamma+1)M_\infty^2\varphi_{xx}-K\}\varphi_x\equiv 0 \tag{2.13}$$

This means that Maeder's linearization is perfectly valid, or that there is no obstacle.

§ 3. Approximate Solution

The approximate equation (2.12) near the obstacle can be easily integrated to give

$$g_x=-\left\{\varphi_x-\frac{1-M_\infty^2}{(\gamma+1)M_\infty^2}\right\}\pm\sqrt{\left\{\varphi_x-\frac{1-M_\infty^2}{(\gamma+1)M_\infty^2}\right\}^2-2\int_c^x\left\{\varphi_{xx}-\frac{K}{(\gamma+1)M_\infty^2}\right\}\varphi_x dx} \tag{3.1}$$

in which the double sign should be taken according as

$$\varphi_x-\frac{1-M_\infty^2}{(\gamma+1)M_\infty^2}\gtrless 0 \tag{3.2}$$

in order to satisfy the condition (2.13). It can readily be seen that g_x also satisfies the boundary condition at lateral infinity ($y\to\pm\infty$ or $r\to\infty$), since φ tends to zero there. The unknown constants c and K are uniquely determined in the following way.

First, g_x will in general be discontinuous at a point where

$$\varphi_x-\frac{1-M_\infty^2}{(\gamma+1)M_\infty^2}=0, \tag{3.3}$$

But, from the physical point of view, any accelerating discontinuity of the flow velocity must be forbidden, so that we should have

$$g_x(c^*)=0 \tag{3.4}$$

where $x=c^*$ is the point satisfying (3.3) in the accelerated flow region. This gives

$$c=c^* \tag{3.5}$$

Secondly, we know $\varphi_x(c^*)=\Phi_x(c^*)$ from (2.4) and (3.4). Together with (2.6) and (3.3), this means that c^* is the sonic point and it is the same for the original linearized flow as for the corrected flow. This is in agreement with Oswatitsch's[3] inference that the linearized transonic flow field would be valid in the neighbourhood of the sonic point at least on the obstacle. Therefore it may be expected that the best agreement of (2.1) and (2.2) would occur in the neighbourhood of $x=c^*$. Hence it is natural to take

$$K=(\gamma+1)M_\infty^2\Phi_{xx}(c^*)=(\gamma+1)M_\infty^2\varphi_{xx}(c^*) \tag{3.6}$$

Thus, the solution Φ_x valid near the obstacle is completely determined as

$$\Phi_x=\frac{1-M_\infty^2}{(\gamma+1)M_\infty^2}\pm\sqrt{Y(x)} \tag{3.7}$$

where

$$Y(x)=\left\{\varphi_x-\frac{1-M_\infty^2}{(\gamma+1)M_\infty^2}\right\}^2-2\int_{c^*}^x\left\{\varphi_{xx}-\frac{K}{(\gamma+1)M_\infty^2}\right\}\varphi_x dx \tag{3.8}$$

$$=\left\{\frac{1-M_\infty^2}{(\gamma+1)M_\infty^2}\right\}^2+\varphi_x^2(c^*)-2\frac{1-M_\infty^2}{(\gamma+1)M_\infty^2}\varphi_x(x)+2\frac{K}{(\gamma+1)M_\infty^2}\{\varphi(x)-\varphi(c^*)\} \tag{3.9}$$

the double sign corresponding to $\varphi_x(x)\gtrless(1-M_\infty^2)/(\gamma+1)M_\infty^2$.

It is interesting to note that the proposal of (3.6) satisfies the two remarkable requirements. The one is that it can also assure the continuous connection with Prandtl-Glauert's theroy at the critical Mach number as well as Maeder's proposal, since then we have $K=0$. The other is an essential analytical behaviour that the square root in (3.8) or (3.9) must not be imaginary.

Indeed we have, from (3.8),

$$dY/dx=2\{\varphi_{xx}(c^*)\varphi_x(x)-\varphi_x(c^*)\varphi_{xx}(x)\} \tag{3.10}$$

$$d^2Y/dx^2=2\{\varphi_{xx}(c^*)\varphi_{xx}(x)-\varphi_x(c^*)\varphi_{xxx}(x)\} \tag{3.11}$$

with the aid of (3.3) and (3.6). Hence

$$Y(c^*)=0, \qquad Y'(c^*)=0 \tag{3.12}$$

and

$$Y''(c^*)=2\{[\varphi_{xx}(c^*)]^2-\varphi_x(c^*)\varphi_{xxx}(c^*)\} \tag{3.13}$$

But, if we confine ourselves to the transonic case such that $\varphi_x(c^*)\cong 0$, we should have $Y''(c^*)>0$. From this and (3.12) we have

$$Y(x)\geqq 0 \tag{3.14}$$

in the neighbourhood of the sonic point $x=c^*$. Further it seems to the author that the relation (3.14) will be generally valid for the main portion on the obstacle. But, in case it breaks down, for example in the neighbourhood of the nose and tail of the body of revolution in the supersonic flow, φ_x as given by the linearized transonic flow theory will give rather good approximation there.

§4. Physical Implications

1) *Sonic Point Behaviour*

In the present method, the sonic point c^* is determined simultaneously with K by the equations:

$$\frac{1-M_\infty^2}{(\gamma+1)M_\infty^2}=\varphi_x(c^*;\ K) \tag{4.1}$$

$$\frac{K}{(\gamma+1)M_\infty^2}=\varphi_{xx}(c^*;\ K). \tag{4.2}$$

Above the free stream critical Mach number, $K\geqq 0$ and c^* moves monotonically forward with increasing Mach number.

In the present approximation, freezing of the flow field at $M_\infty=1$ cannot be accounted for, though the sonic point behaviour with increasing M_∞ for the entire transonic range is qualitatively more reasonably given by this than by any other one single approximation method. In Fig. 1, the sonic point behaviour of a symmetrical circular-arc aerofoil is shown and is compared with the results by Maeder*) and Spreiter[2] (the integral equation method) and with experiments by Bryson[9] and Kawamura[10].

2) *Transonic Normal Shock Wave*

In some cases, (3.3) has another root c^{**} which is in the decelerated flow region. Then,

*) This result was calculated by the author according to Maeder's theory (by use of (A 1) and (A 2)). Then it is remarkble that in the flow with ξ_∞ below $-(2/\pi)^{2/3}$, K vanishes so that there is no drag, while in the present method K does not vanish for ξ_∞ over the critical value, $-(4/\pi)^{2/3}$. The detailed explanation about the reason will be performed in the author's later paper. (see the third paper) Here ξ_∞ is a transonic similarity parameter, $(M_\infty^3-1)/[(\gamma+1)tM_\infty]^{2/3}$, defined by Spreiter.

as is known from (3.7), the flow velocity has a finite discontinuous jump of equal amount $\sqrt{Y(c^{**})}$ from the sonic velocity at the point $x=c^{**}$ which may be quantitatively interpreted as a transonic normal shock wave. Appearance of such an irregular point is due to the quadratic behaviour of g_x in (2.12) and hence in (2.5) as well as in the case of the integral equation method.

It appears usually in the supercritical flow, but arrives at the trailing edge when $M_\infty=1$ in the two-dimensional biconvex case, as is assured by investigating the behaviour of φ_x.

3) *Limiting Form of Φ_x*

We have so far considered the transonic case such that the root of (3.3) exists. But it is also possible to predict the asymptotic approach to the sub- or supersonic linear theory as M_∞ tends to zero or infinity.

In order to achieve the continuty of our transonic solution to the sub- and supersonic solutions through the lower and upper critical Mach numbers respectively, we adopt the following prescriptions to determine the values of c and K, when the real root of (3.3) does not exist. For the subsonic case, (either two-dimensional or axisymmetric), c is taken to be the critical value c^* corresponding to the lower critical Mach number, which corresponds to the point of maximum flow velocity for the incompressible flow. On the other hand, for the two-dimensional supersonic case, we take $c\equiv c^*=0$, that means the leading edge. (It is not necessary to consider the axisymmetric supersonic case.) And hence K is uniquely given by (3.6).

With these extended definitions, the limiting form of Φ_x is obtained as

$$\Phi_x=\varphi_x(x)+\frac{(\gamma+1)M_\infty^2}{2(1-M_\infty^2)}\{\varphi_x^2(x)-\varphi_x^2(c^*)\}-\frac{K}{1-M_\infty^2}\{\varphi(x)-\varphi(c^*)\} \tag{4.3}$$

since the last term in (3.9) tends to zero as $M_\infty\to 0$ or ∞, and

$$\frac{|M_\infty-1|}{(\gamma+1)M_\infty^2}\gg|\varphi_x| \tag{4.4}$$

in the sense of small perturbation. Of course φ itself tends to the conventional sub- or supersonic linear potential.

In consequence, the final formula (3.7) is still valid throughout the whole Mach number range.

§ 5. Examples of Sonic Flow ($M_\infty=1$)

In the case of the sonic flow, Maeder's formal solution for φ can be expressed in the following simple form, on and near the obstacle.

For the two-dimensional flow past a thin symmetrical aerofoil:

$$\varphi(x,\,r)=-\frac{1}{\sqrt{\pi K}}\sum_{n=0}^{1}\frac{(-1^n)}{n!}F^{(n+1)}(x)\frac{x^{n+(1/2)}}{2n+1}+\frac{1}{2}|y|F'(x)+O(t^3),\qquad 0<x<1 \tag{5.1}$$

For the axisymmetric flow past a slender body of revolution:

$$\varphi(x,\,r)=\frac{1}{4\pi}F'(x)\log\frac{e^C K r^2}{4x}-\frac{1}{4\pi}\sum_{n=1}^{1}F^{(n+1)}(x)\frac{(-1)^n}{n\cdot n!}x^n+O(t^4\log t),\qquad 0<x<1 \tag{5.2}$$

where $F(x)$ is the cross-sectional area of the obstacle whose length is $L=1$, and C is Euler's constant. (see Appendix.)

A circular-arc aerofoil of thickness t is approximately given by $|y|=s(x)=2t(x-x^2)$, $0\leqq x\leqq 1$, and hence

$$F(x)=2s(x)=4t(x-x^2),\qquad 0\leqq x\leqq 1 \tag{5.3}$$

Similarly, for the circular-arc body of revolution we have

$$F(x)=\pi s^2(x)=4\pi t^2(x-x^2)^2,\qquad 0\leqq\alpha\leqq 1 \tag{5.4}$$

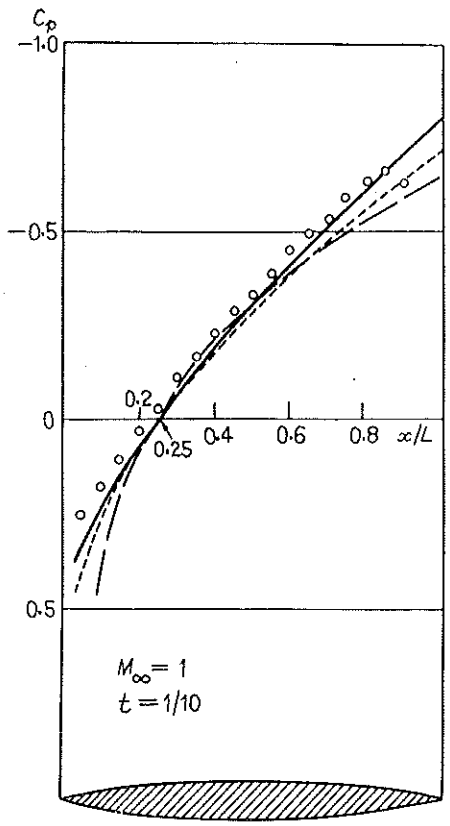

Fig. 2. C_p-distribution on a symmetrical circular-arc aerofoil.

Experiment ○ by Michel, Marchaud and Le Gallo
Theory —— by the present method
– – by Maeder
------ by Spreiter (the local linearization method)

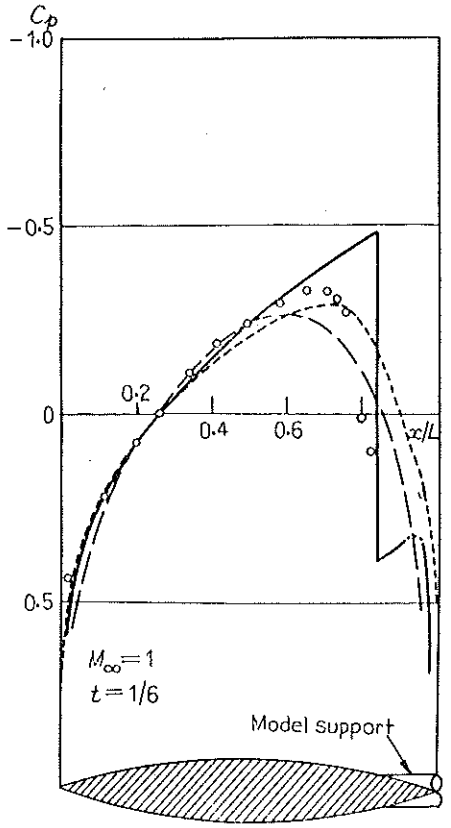

Fig. 3. C_p-distribution on a circular-arc body of revolution.

Experiment ○ by Drougge
Theory —— by the present method
– – by Maeder
------ by Spreiter (the local linearization method)

Calculating Φ_x straightforwardly by the prescribed method, and using the usual approximate expression for the pressure coefficient C_p, we can obtain the distributions of C_p on the above described obstacles of $t=0.1$ and $t=1/6$ respectively, as in Figs. 2 and 3. It will be seen that the present results are the most satisfactory among the various theoretical results, in view of the agreement with the experimental ones by Michel, Marchaud and Le Gallo[11] and Drougge[12]. In Fig. 3, the curve has been corrected near the nose and tail, taking account of the fact described in § 3.*

It is noted in particular that a transonic normal shock wave stays on the axisymmetric body and its nose and tail are the stagnation points. But as viscous effect destroy such a

* The details of the correction are as follows: the proposed method is applied without amy modification to the main portion of the body ($x=0.15\sim0.9$) and the pressure distribution there, which contributes mostly to the total drag, is calculated with the aid of the usual expression of C_p for the axisymmetric body in the small perturbation theory; while in the vicinity of the nose and the tail, where the method is anticipated to fail gradually, φ_x itself is employed in place of Φ_x becaus the former is considered to be more reasonable in the analytical behaviour than the latter, which does not necessarily tend to real minus infinity as should be expected in the axisymmetric case from the viewpoint of the linearized theory. The continuation of the C_p-curve at the front part of the body is very good; but at the rear part does not seem to be so smooth, so that interpolation of some kind for rounding off a sharp corner at the point of connection has to be made.

shock wave on the obstacle, any quantiative discussion about it seems to be without physical significance.

§ 6. Conclusion

The present method is essentially a refinement of the linearzed transonic flow theory, such that the nonlinear characteristics of the fundamental equation is taken into account and the unambiguous determination of the value of K can be made. Also it has an advantage over the integral equation method in simplicity and applicability and over Spreiter's local linearization method in covering the two-dimensional high subsonic flow with a normal shock wave standing on the obstacle as well.

Since our method starts from the linearized transonic flow equation, any solution can be constructed by superposition even in the lifting case, although the final velocity Φ_x for a definite K is no longer superposable. Therefore this method is expected to be the most practical of the existing approximate methods for the transonic flow.

Acknowledgements

The author wishes to express his sincere gratitude to Prafessor I. Imai, his co-researchers and to Professor R. Kawamura for their valuable discussions and continual encouragements. He is also deeply indebted to Dr. M. Yamanouchi, Mr. T. Shigemi and Mr. T. Murasaki for their kind support given to this study at the National Aeronautical Laboratory of Japan.

The author is particularly grateful to Dr. John R. Spreiter of Ames Research Center, N.A.S.A., for his encouragement and instructive comments upon this work.

Appendix

The original linearized transonic potentials corresponding to (2.3) are

$$\varphi(x,y)=-\frac{1}{2\pi}\int_0^1 F'(\xi)e^{\alpha(x-\xi)}\frac{K_0[\alpha\{(x-\xi)^2+\beta^2y^2\}^{1/2}]}{\beta}d\xi, \qquad M_\infty\leqq 1 \qquad \text{(A1)}$$

$$=-\frac{1}{2}\int_0^{x-m|y|} F'(\xi)e^{\alpha(x-\xi)}\frac{I_0[|\alpha|\{(x-\xi)^2-m^2y^2\}^{1/2}]}{m}d\xi, \qquad M_\infty\geqq 1 \qquad \text{(A2)}^*$$

and

$$\varphi(x,r)=-\frac{1}{4\pi}\int_0^1 F'(\xi)e^{\alpha(x-\xi)}\frac{\exp[-\alpha\{(x-\xi)^2+\beta^2r^2\}^{1/2}]}{\{(x-\xi)^2+\beta^2r^2\}^{1/2}}d\xi, \qquad M_\infty\leqq 1 \qquad \text{(A3)}$$

$$=-\frac{1}{2\pi}\int_0^{x-mr} F'(\xi)e^{\alpha(x-\xi)}\frac{\cosh[\alpha\{(x-\xi)^2-m^2r^2\}^{1/2}]}{\{(x-\xi)^2-m^2r^2\}^{1/2}}d\xi, \qquad M_\infty\geqq 1 \qquad \text{(A4)}$$

where K_0 and I_0 are the modified Bessel functions of the zeroth order, and α, β and m are connected with one another as follows,

$$\alpha=\frac{K}{2\beta^2}=-\frac{K}{2m^2}, \qquad \beta^2=1-M_\infty{}^2=-m^2 \qquad \text{(A5)}$$

These potentials can be integrated out on and near the obstacle as follows.

$$\varphi(x,y)=-\frac{1}{2\sqrt{\pi K}}\int_0^x F'(x)\frac{\exp[-Ky^2/4(x-\xi)]}{\sqrt{x-\xi}}d\xi \qquad \text{(A6)}$$

as $M_\infty\to 1\pm 0$. With the substitution,

$$\frac{Ky^2}{4(x-\xi)}=u^2, \qquad \frac{d\xi}{x-\xi}=2\frac{du}{u} \qquad \text{(A7)}$$

and by the Taylor expansion of $F'(x-Ky^2/4u^2)$,

$$\varphi(x,y)=-\frac{|y|}{2\sqrt{\pi}}\sum_{n=0}^{\infty}\frac{(-1)^n}{n!}F^{(n+1)}(x)\left(\frac{Ky^2}{4}\right)^n\int_{(Ky^2/4x)^{1/2}}^{\infty}\frac{e^{-u^2}}{u^{2(n+1)}}du, \qquad 0<x<1 \qquad \text{(A8)}$$

* The expression (A2) is somewhat different form Maeder's one, but the latter is not correct.

Integrations in (A8) can be much simplified by the recurrence relation,

$$J_{n+1}=\frac{2^{2(n+1)}(n+1)!}{\{2(n+1)\}!}\left\{\sum_{k=0}^{n}(-1)^k\frac{\{2(n-k)\}!}{(n-k)!\,2^{2(n-k)+1}}\frac{\exp(-Ky^2/4x)}{(Ky^2/4x)^{n-k+(1/2)}}+(-1)^{n+1}J_0\right\} \tag{A9}$$

where

$$J_n=\int_{(Ky^2/4x)^{1/2}}^{\infty}\frac{e^{-u^2}}{u^{2n}}du,\quad n\geqq 0\quad\text{and}\quad J_0=\frac{\sqrt{\pi}}{2}+O(|y|). \tag{A10}$$

The linear term with respect to $|y|$ in J_0 does not influence that in the following formula (A11). Thus,

$$\varphi(x,r)=-\frac{1}{\sqrt{\pi K}}\sum_{n=0}\frac{(-1)^n}{n!}F^{(n+1)}(x)\frac{x^{n+(1/2)}}{2n+1}+\frac{1}{2}|y|F'(x)+O(t^3),\qquad 0<x<1 \tag{A11}$$

(2) The expressions (A3) and (A4) tend to

$$\varphi(x,r)=-\frac{1}{4\pi}\int_0^x F'(\xi)\frac{\exp[-Kr^2/4(x-\xi)]}{x-\xi} \tag{A12}$$

as $M_\infty\to 1\pm 0$. With the substitution similar to the previous case,

$$\frac{Kr^2}{4(x-\xi)}=u,\qquad \frac{d\xi}{x-\xi}=\frac{du}{u} \tag{A13}$$

and by the Taylor expansion of $F'(x-Kr^2/4u)$,

$$\varphi(x,r)=-\frac{1}{4\pi}\sum_{n=0}\frac{(-1)^n}{n!}F'^{(n+1)}(x)\left(-\frac{Kr^2}{4}\right)^n\int_{Kr^2/4x}^{\infty}\frac{e^{-u}}{u^{n+1}}du,\qquad 0<x<1. \tag{A14}$$

The recurence formula is in this case

$$J_{n+1}=\frac{1}{n!}\left[\sum_{k=0}^{n-1}(-1)^k(n-k-1)!\frac{\exp(-Kr^2/4x)}{(Kr^2/4x)^{n-k}}+(-1)^nJ_1\right],\qquad n\geqq 1 \tag{A15}$$

where

$$\left.\begin{aligned}&J_n=\int_{Kr^2/4x}^{\infty}\frac{e^{-u}}{u^n}\\ \text{and}\quad&J^1=\mathrm{Ei}\left(\frac{Kr^2}{4x}\right)=-C-\log\frac{Kr^2}{4x}+\frac{Kr^2}{4x}+O\left\{\left(\frac{Kr^2}{4x}\right)^2\log\frac{Kr^2}{4x}\right\}\end{aligned}\right\} \tag{A16}$$

Consequently,

$$\varphi(x,r)=\frac{1}{4\pi}F'(x)\log\frac{e^CKr^2}{4x}-\frac{1}{4\pi}\sum_{n=1}F^{(n+1)}(x)\frac{(-1)^n}{n\cdot n!}x^n+O(t^4\log t),\qquad 0<x<1. \tag{A17}$$

It is obvious that the both expressions (A11) and (A17) satisfy the linear boundary conditions on the obstacles.

References

1) J. R. Spreiter and A. Y. Alksne: NACA Tech. Rep. 1217 (1955).
2) J. R. Spreiter and A. Y. Alksne: NACA Tech. Note 4148 (1958).
3) K. Oswatitsch and F. Keune: Proc. Conf. on High Speed Aeronautis, Polytech. Inst. Brooklyn (1955).
4) P. F. Maeder and H. U. Thommen: J. Aero. Sci. **23** (1956) 187.
5) J. W. Miles: J. Aero. Sci. **23** (1956) 704.
6) J. R. Spreiter and A. Y. Alksne: NACA Tech. Rep. 1359 (1958).
7) J. R. Spreiter and A. Y. Alksne: NASA Rep. 2 (1959).
8) K. G. Guderley: *Theorie Schallnaher Strömungen* (Springer, 1957) 33.
9) A. E. Bryson: NACA Tech. Rep. 1984 (1952).
10) R. Kawamura and K. Karashima: Read at the 13th Annual Meeting of Phys. Soc. Japan, Oct. 1958.
11) R. Michel, F. Marchaud and J. Le Gallo: ONERA, Publication no. 65 (1953).
12) G. Drougge: Proc. 9th Intern. Congr. Appl. Mech., vol. 2 (1957) 70.

Transonic Flow past a Wavy Wall*

Transonic flow past an infinitely long sinusoidal wall has not hitherto been thoroughly investigated, although some studies of the high subsonic flow near critical have been made by Kaplan and others by use of the thin-wing-expansion method and the transonic approximation method. In this paper the author studied transonic flows past a sinusoidal wall including shock waves by use of his new method, and could find the velocity and pressure distributions on the wall with success. The result gives a reasonable model for understanding the transition of the flow pattern from subsonic to supersonic.

§1. Introduction

In order to investigate the problem of the existence or non-existence of continuous mixed flows, it seems to be very convenient to study the transonic flow past a wavy wall. In 1940, Görtler[1] found a continuous solution of a high subsonic flow with local supersonic regions past a kind of wavy wall which is correct up to the third approximation and he conjectured it to be convergent. For the case of an exactly sinusoidal wall, the solution of Imai and Oyama[2] by the thin-wing-expansion method seems to be divergent above the critical Mach number. On the other hand, Kaplan[3] showed on the basis of the transonic approximation that a continuous, symmetrical wave solution would diverge above the critical Mach number. According to him, the critical value of the transonic similarity parameter defined after von Karman is $\xi_{\mathrm{crit},K}=-(0.83244/\pi)^{-2/3}$. Thus the solution of the supercritical flow may be asymmetric and would cease to be continuous.

The present work is concerned with this problem. The author makes use of his new method[4], which will be summarized in the next section. This method can give the reasonable features: shock waves appear whenever mixed flows occur, and the solution tends to the same form as that given by the usual linear theory in the sub- and supersonic extremities. The solution, however, has a weak point in the present problem: shock waves in the real flow are always accompanied by entropy increase, which would destroy periodicity of the flow, while the present hypothetical flow is assumed to be isentropic and periodic. But the present investigation seems to be still significant, because the increase of entropy is comparatively small and the periodicity remains locally.

§2. Summary of the Method

The basic equation of the two-dimensional transonic flow can be written as:[4]

$$(1-M_\infty^2)\Phi_{xx}+\Phi_{yy}=(\gamma+1)M_\infty^2\Phi_x\Phi_{xx} \tag{2.1}$$

where $U_\infty\Phi$ is the perturbation velocity potential, U_∞ and M_∞ are the free stream velocity and Mach number respectively, γ is the ratio of specific heats, and the x-axis is taken in the direction of the free stream.

According to Oswatitsch and Maeder, the approximate potential φ satisfies the linearized equation:

$$(1-M_\infty^2)\varphi_{xx}+\varphi_{yy}=K\varphi_x \tag{2.2}$$

where K is an appropriately chosen constant. The solution of (2.2) can be found in a simple way with the given boundary conditions, apart from the selection of the value of K.

Here we put

$$\Phi=\varphi+g \tag{2.3}$$

* Journal of the Physcical Society of Japan, vol. 15, No. 11, P. 2080~2086, November, 1960.

and establish the equation governing the nonlinear correction term g. Then, with the aid of the order estimation of the equation, g_x can be calculated approximately in the neighbourhood of the boundary and it can be found that g_x and φ_x are of the same order of magnitude. (From this point of view, the linearized theory due to Maeder cannot be of the first order approximation in itself, because of the tacit assumption, $\varphi \gg g$.)

Finally g_x can be integrated as follows:

$$g_x=-\varphi_x+(1-M_\infty^2)/\{(\gamma+1)M_\infty^2)\}\pm\sqrt{Y(x)} \tag{2.4}$$

where

$$Y(x)=\left\{\varphi_x-\frac{1-M_\infty^2}{(\gamma+1)M_\infty^2}\right\}^2-2\int_{c^*}^{x}\left\{\varphi_{xx}-\frac{K}{(\gamma+1)M_\infty^2}\right\}\varphi_x dx \tag{2.5}$$

and the double sign corresponds to

$$\varphi_x \gtrless (1-M_\infty^2)/\{(\gamma+1)M_\infty^2\} \tag{2.6}$$

On the proper physical and mathematical grounds, c^* and K are uniquely determined in the following manner:

$$\varphi_x(x=c^*,\ y=0\ ;\ K)=(1-M_\infty^2)/\{(\gamma+1)M_\infty^2\} \tag{2.7}$$

$$\varphi_{xx}(x=c^*,\ y=0\ ;\ K)=K/\{(\gamma+1)M_\infty^2\} \tag{2.8}$$

The former is the condition that $x=c^*$ is the sonic point on the boundary, and the latter means that K should be taken as the value of the acceleration at the sonic point. In treating usual transonic flows, (2.7) and (2.8) constitute the simultaneous equations for finding c^* and K. Next, for purely subsonic or supersonic flows, the value of c^* should be kept fixed at its lower or upper critical value just when the sonic point disappears out of the flow, on account of the continuous transition of the flow field with changing Mach number. And then K should be determined by (2.8) alone.

§ 3. Linearized Transonic Flow Potential

First we require the solution of (2.2) subject to the boundary conditions:

i) $\varphi_y=f'(x)=i\omega f_0 e^{i\omega x}$, for $y=0$ (3.1)

ii) grad $\varphi\to 0$, for $y\to\infty$ (3.2)

where the wavy boundary is expressed as

$$f(x)=f_0 e^{i\omega x}\ \ (f_0,\ \omega:\ \text{real constants}) \tag{3.3}$$

Here and hereafter we shall consider only the real parts of the complex expressions;

Now this solution is

$$\varphi=-(i\omega f_0/\mu)\exp(-\mu y+i\omega x) \tag{3.4}$$

where

$$\mu=(\beta^4\omega^4+K^2\omega^2)^{1/4}\exp\left(\frac{i}{2}\tan^{-1}\frac{K}{\beta^2\omega}\right) \tag{3.5}$$

$$\beta^2=1-M_\infty^2 \tag{3.6}$$

so that

$$\varphi=-(\omega f_0/|\mu|)\exp[-\mathrm{Re}(\mu)y+i\{\omega x-\mathrm{Im}(\mu)y-\arg(\mu)+\pi/2\}] \tag{3.7}$$

By differentiation we have

$$\varphi_x=(\omega^2 f_0/|\mu|)\exp[-\mathrm{Re}(\mu)y+i\{\omega x-\mathrm{Im}(\mu)y-\arg(\mu)\}] \tag{3.8}$$

$$\varphi_{xx}=(i\omega^3 f_0/|\mu|)\exp\left[-\mathrm{Re}(\mu)y+i\{\omega x-\mathrm{Im}(\mu)y-\arg(\mu)\}\right] \tag{3.9}$$

In (3.8), we can see a rough feature of the transonic flow. First, in a supercritical flow in which $K\neq 0$, the perturbed velocity and so the pressure have a phase lag, $\arg(\mu)$, relative to the wall, which approaches $\pi/2$ as $\beta^2\to-\infty$ so that the solution would agree with that given by the supersonic linear theory. It is interesting to note that $\arg(\mu)$ becomes $\pi/4$ when $M_\infty\to 1\pm 0$. Secondly, as is seen from (3.7)–(3.9), the perturbed wave is propagated along the straight line:

$$y=\{\omega/\mathrm{Im}(\mu)\}x+\text{const.} \tag{3.10}$$

which tends to the Mach line as $\beta^2\to-\infty$, as should be expected.

§4. Procedure of Refinement

1) *Constants c^* and K*

In the present case, (2.7) and (2.8) become

$$(1-M_\infty^2)/\{(\gamma+1)M^2{}_\infty\}=\omega^2 f_0/|\mu|\exp\left[i\{\omega c^*-\arg(\mu)\}\right] \tag{4.1}$$

$$K/\{(\gamma+1)M^2{}_\infty\}=i\omega^3 f_0|\mu|\exp[i\{\omega c^*-\arg(\mu)\}] \tag{4.2}$$

with the aid of (3.8) and (3.9). If we introduce the transonic similarity parameter after Spreiter, $\xi_\infty=(M_\infty^2-1)/[(\gamma+1)M_\infty^2(2f_0)]^{2/3}$, where the wave length is assumed as unity, and another parameter after Maeder $\alpha=K/2\beta^2$, the equation can be simplified as

$$\pm|\xi_\infty|^{3/2}=\frac{\pi}{(1+\alpha^2/\pi^2)^{1/4}}\exp\left[i\left(2\pi c^*-\frac{1}{2}\tan^{-1}\frac{\alpha}{\pi}\right)\right] \tag{4.3}$$

$$\pm 2\alpha|\xi_\infty|^{3/2}=i\frac{2\pi^2}{(1+\alpha^2/\pi^2)^{1/4}}\exp\left[i\left(2\pi c^*-\frac{1}{2}\tan^{-1}\frac{\alpha}{\pi}\right)\right] \tag{4.4}$$

where the double sign corresponds to $M_\infty\lesseqgtr 1$.

Taking the real parts of the above equations, and eliminating $|\xi_\infty|$, we can obtain

$$2\pi c^*=-(1/2)\tan^{-1}(\alpha/\pi) \tag{4.5}$$

and hence the solutions for c^* and α:

$$\cos 4\pi c^*=-\xi_\infty/\pi^{2/3} \tag{4.6}$$

$$\alpha=\pm\pi\sqrt{(\pi^{4/3}/\xi_\infty^2)-1} \tag{4.7}$$

where $|\xi_\infty|\leqq\pi^{2/3}$ is assumed.

Next we know from (4.6) that $\mp\pi^{2/3}$ should be the lower and upper critical values of ξ_∞ respectively and then c^*'s are N and $(-1/4)+N$ where N is an integer. Thus in order to know α in the case of $|\xi_\infty|\geqq\pi^{2/3}$, we have only to fix c^* at these values and solve for α by (4.4) in accordance with the prescription given in §2. As a result, it is assured that $\alpha=0$ holds irrespective of the values of ξ_∞ when $|\xi_\infty|\geqq\pi^{2/3}$.

Consequently we obtain the following explicit expressions of the linearized flow velocity.

$$\varphi_x=(\pi^{2/3}/|\beta|)2f_0|\xi_\infty|^{1/2}\exp\left[i\{2\pi x-(1/2)\tan^{-1}(\pm\sqrt{(\pi^{4/3}/\xi_\infty^2)-1})\}\right] \tag{4.8}$$

$$=\frac{\pi^{2/3}(2f_0)^{2/3}}{(\gamma+1)^{1/3}M_\infty^{2/3}}\exp\left[i\left\{2\pi x-\frac{1}{2}\tan^{-1}\left(\pm\sqrt{\frac{\pi^{4/2}}{\xi_\infty{}^2}-1}\right)\right\}\right] \tag{4.9}$$

$$\text{for}\quad|\xi_\infty|\leqq\pi^{2/3}$$

$$=\{\pi(2f_0)/\beta\}e^{i(2\pi x)}\qquad\text{for}\quad\xi_\infty\leqq-\pi^{2/2} \tag{4.10}$$

$$=\{\pi(2f_0)/|\beta|\}e^{i(2\pi x-\pi/2)}\qquad\text{for}\quad\xi_\infty\geqq\pi^{2/3} \tag{4.11}$$

2) *Sonic Point and Shock Wave Position*

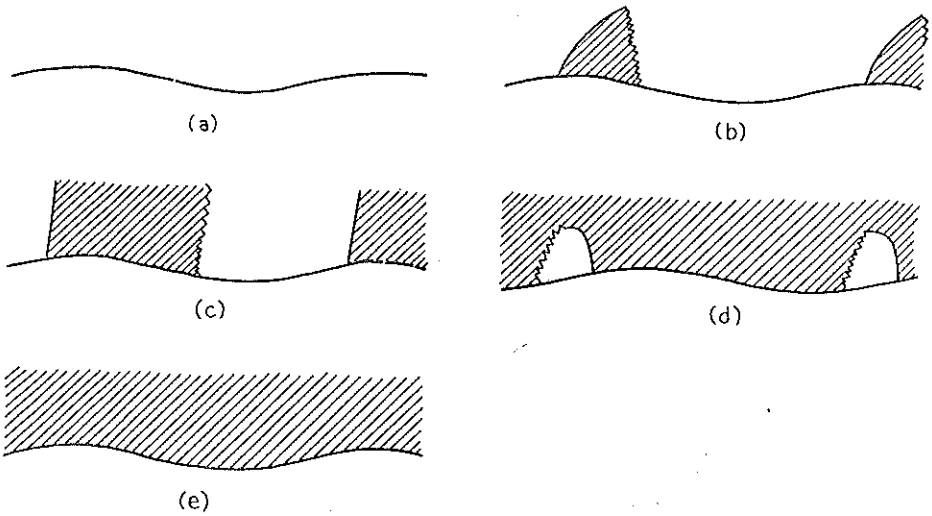

Fig. 1. Pictures of various transonic flows.

(a) subsonic flow.
(b) subsonic supercritical flow.
(c) sonic flow.
(d) supersonic but below upper critical flow.
(e) supersonic flow

Shaded portions indicate supersonic regions, wnich are enclosed by sonic lines and shock lines drawn with solid and saw-toothed lines respectively.

When $|\xi_\infty| \leqq \pi^{2/3}$, we can find another root c^{**} in place of c^* from (4.3) and (4.7) as follows:

$$-\xi_\infty = \pi^{2/3}\cos\{2\pi c^{**} - (1/2)\tan^{-1}(\pm\sqrt{(\pi^{4/3}/\xi_\infty^2)-1})\} \tag{4.12}$$

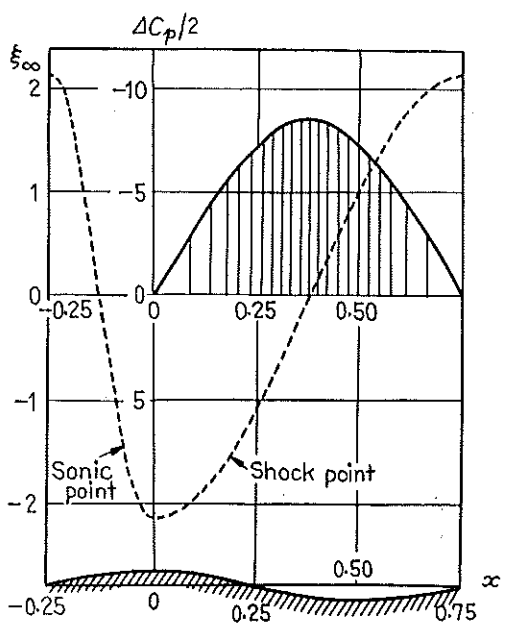

Fig. 2. Movement of sonic point and shock wave position on the wall with varying ξ_∞ and pressure jump at the shock.

$x = c^{**}$ is a point located in the decelerated flow region and it is known from (2.4)–(2.6) that there appears some velocity discontinuity at c^{**}. As was known from the previous paper[4], it is considered as the position of the shock wave on the wall.

The manners in which the sonic point and the shock point on the wall change with ξ_∞ are shown in Fig. 2. Both of them first appear at the summits of the wavy wall at the instant when M_∞ reaches the lower critical value; then the sonic points move upstream and the shock points downstream with increasing Mach number, until each sonic point joins, at the upper critical Mach number, the receding shock point which has originated at the preceding summit of the wavy wall: thus all the sonic points coincide with the shock points and hence the subsonic regions disappear. This result may be interpreted as shown roughly in Fig. 1.

3) *Results of the Procedure of Refinement*

If we write

$$\varphi_x = (2f_0)/|\beta| \cdot N(x;\ \xi_\infty) \tag{4.13}$$

the following expressions for Φ_x are obtained with the aid of (2.4) and (2.5);

$$\Phi_x=\frac{1-M_\infty^2}{(\gamma+1)M_\infty^2}\pm\sqrt{2}\sqrt{\frac{(1-M_\infty^2)^2}{(\gamma+1)^2M_\infty^4}-\frac{(1-M_\infty^2)(2f_0)}{(\gamma+1)M_\infty^2|\beta|}N(x)+\frac{K(2f_0)}{(\gamma+1)M_\infty^2|\beta|}\int_{c^*}^{x}N(x)dx} \tag{4.14}$$

$$=\frac{2f_0}{|\beta|}\left\{(\pm)^1|\xi_\infty|^{3/2}\pm\sqrt{2}\sqrt{|\xi_\infty|^3(\mp)_1|\xi|^{3/2}N(x)+2|\alpha||\xi_\infty|^{3/2}\int_{c^*}^{x}N(x)dx}\right\} \tag{4.15}$$

for $|\xi_\infty|\leqq\pi^{2/3}$

and

$$\Phi_x=\frac{1-M_\infty^2}{(\gamma+1)M_\infty^2}\pm\sqrt{\frac{(1-M_\infty^2)^2}{(\gamma+1)^2M_\infty^4}+\frac{(2f_0)^2}{|\beta|^2}N(c^*)^2-2\frac{(1-M_\infty^2)}{(\gamma+1)M_\infty^2}\left(\frac{2f_0}{|\beta|}\right)N(x)} \tag{4.16}$$

$$=\frac{2f_0}{|\beta|}\{(\pm)_1|\xi|^{3/2}\pm\sqrt{|\xi_\infty|^3+N(c^*)^2(\mp)_12|\xi_\infty|^{3/2}N(x)}\} \tag{4.17}$$

for $|\xi_\infty|\geqq\pi^{2/3}$

where the double signs with and without the parenthesis $(\ )_1$ correspond respectively to $M_\infty\leqq1$ and

$$N(x)(\mp)_1|\xi_\infty|^{3/2}\geqq0 \tag{4.18}$$

Here if the reduced pressure coefficient,

$$\bar{C}_p=\frac{\{(\gamma+1)M_\infty^2\}^{1/3}}{(2f_0)^{2/3}}C_p=\frac{|\beta|}{(2f_0)|\xi_\infty|^{1/2}}C_p \tag{4.19}$$

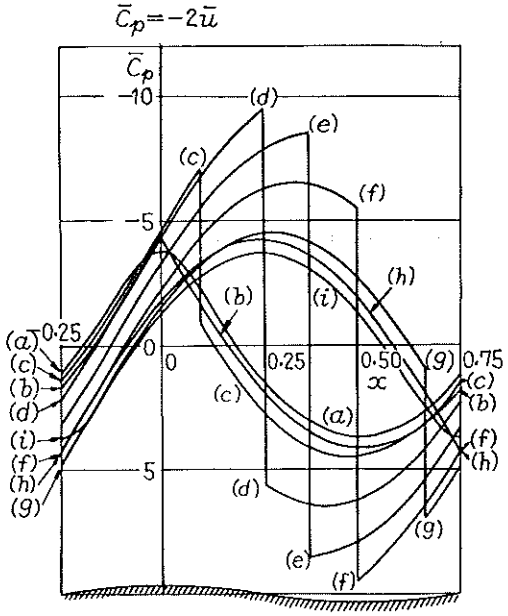

Fig. 3. Pressure distributions on the wall in terms of C_p.

(a)	$\xi_\infty=-2.8$
(b)	$=-\pi^{2/3}$
(c)	$=-2.0$
(d)	$=-1.0$
(e)	$=0$
(f)	$=1.0$
(g)	$=2.0$
(h)	$=\pi^{2/3}$
(i)	$=2.8$

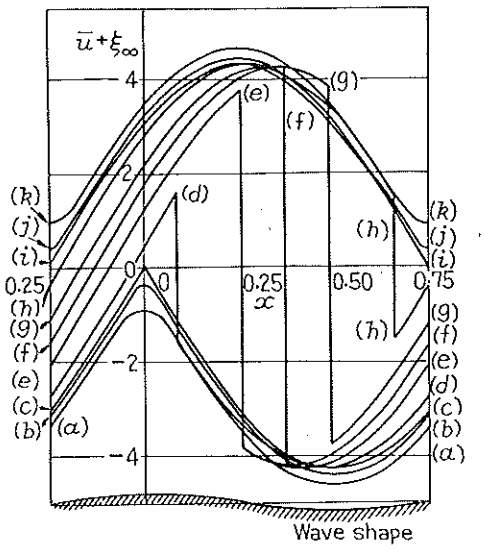

Fig. 4. Velocity distributions on the wall in terms of $\bar{u}+\xi_\infty$.

(a)	$\xi_\infty=-2.8$
(b)	$=-2.4$
(c)	$=-\pi^{2/3}$
(d)	$=-2.0$
(e)	$=-1.0$
(f)	$=0$
(g)	$=1.0$
(h)	$=2.0$
(i)	$=\pi^{2/3}$
(j)	$=2.4$
(k)	$=2.8$

is introduced, we can obtain, using the approximate relation $C_p=-2\Phi_x$,

$$\bar{C}_p=-2\left\{(\pm)_1|\xi_\infty|\pm\sqrt{2}\sqrt{|\xi_\infty|^2(\mp)_1|\xi_\infty|^{1/2}N(x)+2|\alpha||\xi_\infty|^{1/2}\int_{c^*}^{x}N(x)dx}\right\} \tag{4.20}$$

and

$$\bar{C}_p=-2\{(\pm)_1|\xi_\infty|\pm\sqrt{|\xi_\infty|^2+N(c^*)^2|\xi_\infty|^{-1}(\mp)_1 2|\xi_\infty|^{1/2}N(x)}\} \tag{4.21}$$

$$=-2|\xi_\infty|^{1/2}\begin{Bmatrix}e^{i(2\pi x)} & (\xi_\infty<o)\\ e^{i(2\pi x-\pi/2)} & (\xi_\infty>o)\end{Bmatrix}+O(|\xi_\infty|^{-2}) \tag{4.22}$$

$$\text{for } |\xi_\infty|\geqq\pi^{2/3}$$

All these results are consistent with the transonic similarity law.

(4.22) may be rewritten in the usual form of the pressure coefficient as follows:

$$C_p=-2\frac{(2f_0)}{|\beta|}\pi\begin{Bmatrix}e^{i(2\pi x)} & (\xi_\infty<o)\\ e^{i(2\pi x-\pi/2)} & (\xi_\infty>o)\end{Bmatrix}+O[(2f_0)^2] \tag{4.23}$$

This agrees with the result given by the usual linear theory.

Next, in order to see directly the velocity distribution in a reduced form that is invariant under the transonic similarity transformation, we introduce the following quantity;

$$\bar{u}+\xi_\infty\equiv\frac{\{(\gamma+1)M_\infty^2\}^{1/3}}{(2f_0)^{2/3}}\left\{\Phi_x+\frac{M_\infty^2-1}{(\gamma+1)M_\infty^2}\right\}=\frac{M^2-1}{\{(\gamma+1)(2f_0)M_\infty^2\}^{2/3}} \tag{4.24}$$

Then it indicates the local Mach number distribution in such a manner that

$$\bar{u}+\xi_\infty\gtrless 0 \qquad \text{when} \qquad M\gtrless 1 \tag{4.25}$$

Thus we can see our results for the pressure and local Mach number distributions in terms of the respective reduced quantities in Figs. 3 and 4. Now, the half of the pressure jump at the shock is found from (4.20), that is,

$$\Delta C_p/2=2\sqrt{2}\sqrt{|\xi_\infty|^2(\mp)_1|\xi_\infty|^{1/2}N(c^{**})+2|\alpha||\xi_\infty|^{1/2}\int_{c^*}^{c^{**}}N(x)dx} \tag{4.26}$$

which is shown in Fig. 2, for a given shock wave position c^{**}.

§ 5. Discussion and Conclusion

A comparison with Kaplan's result for the lower critical flow is shown in Fig. 5. For the wall of the waviness ratio $2f_0=0.01$, the critical Mach number is about 0.91 in his case, according to Shapiro's sample calculation[5], while it is 0.917 in our case. With respect to the peak negative pressure there is no great difference. Thus, our approximation method is more satisfactory in comparison with Kaplan's one which requires more lengthy calculation, in order to inquire into the general feature of transonic flows.

Further, we can find a close analogy between the flows through a one-dimensional Laval nozzle and past a sinusoidal wall. Namely, the flow patterns shown in Figs. 3 and 4 are quite similar to those of the former if the sonic point of the latter is considered

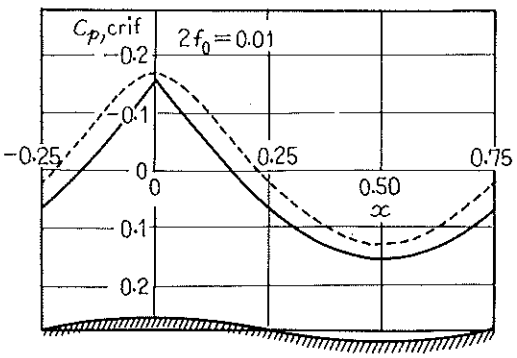

Fig. 5. Comparison of pressure distributions on the wall in the lower critical flow, predicted by Kaplan and by the present method. (The former is based on the figure given in Ref 5.)

------ Kaplan, $M_{\infty,\mathrm{crit}}=0.91$

——— Present, $M_{\infty,\mathrm{crit}}=0.917$

as corresponding to the throat, although in our case the sonic point moves upstraem along the wall with increasing Mach number. Therefore it is not strange that the curves of $\overline{C}_p(x)$ and $\overline{u}(x)+\xi_\infty$ have sharp angles at the sonic points when the flow is critical (lower or upper). It will be interesting to compare this fact with Wood and Clarke's recent work[6] on the transonic flow in cascades, in which they evaluated, with success, the effect of the nonlinear term of the fundamental equation (2–1) by replacing the term by the corresponding quantity of the one-dimensional flow.

Thus, it is found that our new approximation method can be applied successfully to the transonic flow past a sinusoidal wall and hence it may be expected that our method would be useful for the consideration of the general feature of the transonic flows.

In conclusion, the author wishes to express his sincere gratitude to Professor R. Kawamura and Mr. T. Shigemi for their kind advice and valuable discussions.

References

1) H. Görtler: Z. a. M. M. **20** (1940) 254.
2) I. Imai and S. Oyama: Rep. Inst. Sci. Tech., Univ. Tokyo **2** (1948) 39.
3) C. Kaplan: NACA Tech. Note 2748 (1952).
4) I. Hosokawa: J. Phys. Soc. Japan **15** (1960) 149.
5) A. H. Shapiro: *The Dynamics and Thermodynamics of Compressible Fluid Flow* II (Ronald Press. New York, 1954) 841 p.
6) A. D. Wood and J. H. Clarke: J. Aero. Sci. **26** (1959) 318.

Theoretical Prediction of the Pressure Distribution on a Non-lifting, Thin Symmetrical Aerofoil at Various Transonic Speeds*

Theoretical pressure distributions on a non-lifting, circular-arc aerofoil at various transonic speeds are obtained by application of a new method recently published by the author. The method consists essentially of a refinement of the linearized transonic flow theory in which the nonlinear characteristics of the fundamental equation are taken into account. The results reveal most of the principal phenomena observed in experimental studies throughout the whole Mach number range.

§1. Introductory Remarks

Recently, a useful method of analysis on the transonic flows around a thin obstacle was proposed by the author.[1] Its basic idea consists in the correction of the linearized transonic flow theory[2),3)] in which the nonlinearity of the flow field is taken into account. In one of the previous papers,[1] the logical stucture of the theory and the main features deduced from it are described together with two examples of calculation for the sonic flow case ($M_\infty=1$).

The other paper[4] treats the transonic flow past a wavy wall as a simple but interesting example of applications of the theory. The result for the lower critical flow is nearly in agreement with Kaplan's more exact one. Furthermore, it illustrates various flows including shock waves plausible for the higher free-stream Mach numbers.

However, there remains another family of the more important case of the transonic flow, that is, the flow around an isolated aerofoil. In this paper, a symmetrical circular-arc aerofoil is dealt with as a typical example of such problems; first the behaviours of the sonic and shock points on the aerofoil in accordance with the change of the transonic similarity parameter are examined in detail, as a necessary process of the present method, and next, various velocity and pressure distributions on the aerofoil are obtained. Also the pressure drag is plotted against the transonic similarity parameter, and compared with data published by other authors. All the quantities are arranged in the reduced form consistent with the transonic similarity law for the sake of simplicity and convenience of utilization. In the next section, a summarized description of our method is given.

§2. Summary of the Method

The differential equation for the steady, two-dimensional transonic flow is as follows:

$$(1-M_\infty^2)\Phi_{xx}+\Phi_{yy}=(\gamma+1)M_\infty^2\Phi_x\Phi_{xx} \tag{2.1}$$

where $U_\infty\Phi$ is the perturbation velocity potential; γ is the ratio of specific heats; M_∞ and U_∞ are the Mach number and the velocity of the free stream respectively; and the x-axis is taken in the direction of the free stream.

In order to obtain the approximate solution, Oswatitsch[2] and Maeder[3] suggest to deal with the following equation (the linearized transonic flow theory);

$$(1-M_\infty^2)\varphi_{xx}+\varphi_{yy}=K\varphi_x \tag{2.2}$$

in which K is a constant having the meaning of the acceleration at a certain point of the flow field, as is known from comparison of (2.1) and (2.2).

Now it has been derived in the previous paper[1] that a more exact solution of (2.1) based upon reasonable assumptions could be obtained provided the solution of the linearized equation

* Journal of the Physical Society of Japan, Vol. 16, No. 3, P. 546~558, March, 1961.

(2.2), $\varphi(x\,;\,K)$, were found. The procedure of refinement can be written as follows:

$$\Phi_x=(1-M_\infty{}^2)/[(\gamma+1)M_\infty{}^2]\pm\sqrt{Y(x)} \tag{2.3}$$

where

$$Y(x)=\left\{\frac{1-M_\infty{}^2}{(\gamma+1)M_\infty{}^2}\right\}^2+\varphi_x{}^2(c^*)-2\frac{1-M_\infty{}^2}{(\gamma+1)M_\infty{}^2}\varphi_x(x)+2\frac{K}{(\gamma+1)M_\infty{}^2}\{\varphi(x)-\varphi(c^*)\} \tag{2.4}$$

and the double sign corresponds to

$$\varphi_x\lessgtr(1-M_\infty{}^2)/[(\gamma+1)M_\infty{}^2] \tag{2.5}$$

respectively. In the above equation, the unknown constants c^* and K should be determined according to the following prescriptions;

$$1-M_\infty{}^2=(\gamma+1)M_\infty{}^2\varphi_x(c^*\,;\,K) \tag{2.6}$$

$$K=(\gamma+1)M_\infty{}^2\varphi_{xx}(c^*\,;\,K) \tag{2.7}$$

The both constitute the simultaneous algebraic equations for c^* and K in case of usual transonic flow. The former represents that $x=c^*$ is the sonic point on the surface of the aerofoil. If (2.6) has more than one root for c^*, $x=c^*$ must be the sonic point in the accelerated region of the flow. The latter equation, on the other hand, serves in determining $K(>0)$ as equal to the acceleration of the flow at the sonic point on the aerofoil. In case of purely sub- or supersonic flow, (2.6) has no root; but also in this case c^* should take the solution from transonic to sub- or supersonic, and then K is determined by (2.7) for this value of c^*.

Finally, we shall now enumerate some characteristic features of our approach:[1]

1) The constant K is uniquely determined and there is no such ambiguity as is seen in the linearized transonic flow theory.

2) The occurrence of shock is predicted as the discontinuities in the pressure and velocity on the surface.*

3) The procedure of approximation is very simple, because it does not require any assumption or knowledge about the entire flow field and the whole shape of the sonic and shock lines; nevertheless the results obtained by the method are reliable, in so far as our estimation is valid on the order of magnitude of various quantities in the neighbourhood of the obstacle.

§ 3. The Linearized Transonic Flow

According to Maeder's theory, the formal solutions of (2.2) representing the linearized transonic flow past a thin, symmetrical aerofoil are written as follows;

$$\varphi(x,\ y)=-\frac{1}{2\pi}\int_0^1 F'(\xi)\frac{e^{\alpha(x-\xi)}}{\beta}K_0(\alpha\sqrt{(x-\xi)^2+\beta^2y^2}\,)\xi d,\quad M_\infty\leqq 1 \tag{3.1}$$

$$\varphi(x,\ y)=-\frac{1}{2}\int_0^{x-my} F'(\xi)\frac{e^{\alpha(x-\xi)}}{m}I_0(|\alpha|\sqrt{(x-\xi)^2-m^2y^2}\,)d\xi,\qquad M_\infty\geqq 1 \tag{3.2}$$

where α, β and m are related to each other as

$$\beta^2=1-M_\infty{}^2=-m^2,\quad \alpha=K/2\beta^2\,; \tag{3.3}$$

$F(x)$ is the cross-sectional area of the aerofoil, whose chord length can be assumed unity without loss of generality, the origin of the co-ordinate being at the leading edge; and K_0 and I_0 are the modified Bessel functions of the zeroth order.

* Though it is not affirmed from the standpoint of the exact treatment of the problem (Lin and Rubinov[5]) that a normal shock wave stays on the curved surface, it may be admitted for an approximate treatment.

1) *Subsonic case* ($M_\infty \leqq 1$)

On the aerofoil, we can have the limit:

$$\lim_{y\to 0}\varphi(x,\ y)=-\frac{1}{2\pi}\int_0^1 F'(\xi)\frac{e^{\alpha(x-\xi)}}{\beta}K_0(\alpha|x-\xi|)d\xi \tag{3.4}$$

since the integral is uniformly covergent when y tends to zero. Thus, its derivative is

$$\lim_{y\to 0}\varphi_x=\frac{1}{2\pi\beta}\int_0^1 F'(\xi)\frac{\partial}{\partial\xi}\{e^{\alpha(x-\xi)}K_0(\alpha|x-\xi|)\}d\xi \tag{3.5}$$

$$=\frac{1}{2\pi\beta}\left\{F'(\xi)e^{\alpha(x-\xi)}K_0(\alpha|x-\xi|)\Big|_{\xi=0}^{\xi=1}-\int_0^1 F''(\xi)e^{\alpha(x-\xi)}K_0(\alpha|x-\xi|)d\xi\right\}. \tag{3.6}$$

If $F(\xi)$ is expressed by a polynomial (which means a sharp-edged aerofoil), we can express $F''(\xi)$ with a power series:

$$F''(\xi)=\sum_{n=0} a_n\xi^n \tag{3.7}$$

and the integral in (3.6) can be reduced to the following forms:

$$J_n=\int\xi^n e^{\alpha(x-\xi)}K_0(\alpha|x-\xi|)d\xi,\qquad n=0,\ 1,\cdots, \tag{3.8}$$

The integration can conveniently be carried out by taking account of Schläfli's integrals of of Poisson's type for the modified Bessel functions[14] and their derivatives:

$$z^{-\nu}K_\nu(z)=z^{-\nu}K_{-\nu}(z)=\frac{\Gamma(1/2)}{2^\nu\Gamma(\nu+1/2)}\int_1^\infty e^{-zt}(t^2-1)^{\nu-1/2}dt \tag{3.9}$$

$$\frac{d}{dz}[z^{-\nu}K_{-\nu}(z)]=-\frac{\Gamma(1/2)}{2^\nu\Gamma(\nu+1/2)}\int_1^\infty te^{-zt}(t^2-1)^{\nu-1/2}dt. \tag{3.10}$$

First, we shall deal with J_0:

$$J_0=\int e^{\alpha(x-\xi)}K_0(\alpha|x-\xi|)d\xi=\int_1^\infty(t^2-1)^{-1/2}dt\int e^{\alpha(x-\xi)-\alpha|x-\xi|t}d\xi \tag{3.11}$$

$$=\int_1^\infty(t^2-1)^{-1/2}\frac{e^{\alpha(x-\xi)(1\mp t)}}{-\alpha(1\mp t)}dt$$

$$=-\frac{1}{\alpha}e^{\alpha(x-\xi)}\left\{-\int_1^\infty e^{-\alpha|x-\xi|t}(t^2-1)^{-3/2}dt\mp\int_1^\infty te^{-\alpha|x-\xi|t}(t^2-1)^{-3/2}dt\right\}$$

$$=-\frac{1}{\alpha}e^{\alpha(x-\xi)}\left\{\alpha|x-\xi|K_1(\alpha|x-\xi|)\mp\frac{d}{d(\alpha|x-\xi|)}\alpha|x-\xi|K_1(\alpha|x-\xi|)\right\} \tag{3.12}$$

in which the double sign corresponds to $x\leqq\xi$, respectively. Thus we get

$$J_0=-e^{\alpha(x-\xi)}\{|x-\xi|K_1(\alpha|x-\xi|)+(x-\xi)K_0(\alpha|x-\xi|)\} \tag{3.13}$$

by use of the relation $d/dz(zK_1(z))=-zK_0(z)$. In a general case of J_n, a similar procedure leads to the result which includes the modified Bessel functions of the higher order with the aid of (3.9) and (3.10).

For a circular-arc aerofoil which is certainly the simplest case, we can obtain the following integrated expression of (3.1), taking account of $F(\xi)=4t(\xi-\xi^2)$ ($F''(\xi)=-8t$) and (3.13);

$$\varphi_x=\frac{4t}{\pi\beta}\left[e^{\alpha(x-\xi)}\left\{\left(\frac{1}{2}-x\right)K_0(\alpha|x-\xi|)-|x-\xi|K_1(\alpha|x-\xi|)\right\}\right]_{\xi=0}^{\xi=1} \tag{3.14}$$

or

$$=\frac{4t}{\pi\beta}\left[e^{\alpha(x-1)}\left\{\left(\frac{1}{2}-x\right)K_0[\alpha(1-x)]-(1-x)K_1[\alpha(1-x)]\right\}\right.$$

$$-e^{\alpha x}\left\{\left(\frac{1}{2}-x\right)K_0(\alpha x)-xK_1(\alpha x)\right\}\Bigg]. \tag{3.15}$$

In the limit, $\alpha\to\infty$ and $\beta\to 0$ ($M_\infty=1-0$), (3.15) becomes

$$\varphi_x=-\frac{2t}{\sqrt{\pi K}}(x^{-1/2}-4x^{1/2}) \tag{3.16}$$

as was already proved by another way in the previous work.[1)]

Differentiation of (3.15) gives

$$\varphi_{xx}=\frac{4t}{\pi\beta}\Bigg[e^{\alpha(x-1)}\left\{\left(-\frac{1}{2}\alpha-1\right)K_0[\alpha(1-x)]-\frac{1}{2}\alpha K_1[\alpha(1-x)]\right.$$
$$\left.-e^{\alpha x}\left\{\left(\frac{1}{2}\alpha-1\right)K_0(\alpha x)-\frac{1}{2}\alpha K_1(\alpha x)\right\}\Bigg]. \tag{3.17}$$

In Maeder's theory K should be determined as follows;

$$K=(\gamma+1)M_\infty{}^2\varphi_{xx}\left(x=\frac{1}{2};\ K\right). \tag{3.18}$$

After rearranging this equation, we get

$$\frac{\pi}{2}(-\xi_\infty)^{3/2}\left(\frac{\alpha}{2}\right)=\left(\sinh\frac{\alpha}{2}-\frac{\alpha}{2}\cosh\frac{\alpha}{2}\right)K_0\left(\frac{\alpha}{2}\right)+\frac{\alpha}{2}\sinh\frac{\alpha}{2}K_1\left(\frac{\alpha}{2}\right). \tag{3.19}$$

We know from this equation that $\alpha/2$ has a non-vanishing solution only when $(\pi/2)(-\xi_\infty{}^{3/2})<1$, that is, $-(2/\pi)^{2/3}<\xi_\infty<0$. In addition to that, the equation has a trivial solution $\alpha=0$ for all negative values of ξ_∞. Thus the point $\xi_\infty=-(2/\pi)^{2/3}$ makes a branch point on the diagram of ξ_∞ versus α, or ξ_∞ versus c^*, as is seen in Fig. 1. Within the range between $-(2/\pi)^{2/3}<\xi_\infty<0$, we must of course adopt the finite solution since the significant characteristics of the transonic flow are given only by the non-vanishing solution of $\alpha/2$ or K; in the other range, however, the solution $\alpha=0$ is useful, which provides Prandtl-Glauert's approximation in itself. Maeder's theory is interesting in that it leads to an existence of a symmetric solution ($\alpha=0$) which results in no pressure drag even at the supercritical state ($\xi_\infty>-(4/\pi)^{2/3}$, which is derived from (3.15)).

2) *Supersonic case* ($M_\infty\geqq 1$)

After the treatment similar to the previous case, we have

$$\lim_{y\to 0}\varphi(x,y)=-\frac{1}{2}\int_0^x F'(\xi)\frac{e^{\alpha(x-\xi)}}{m}I_0[|\alpha|(x-\xi)]d\xi \tag{3.20}$$

$$\lim_{y\to 0}\varphi_x=-\frac{1}{2m}F'(x)+\frac{1}{2m}\int_0^x F'(\xi)\frac{\partial}{\partial\xi}e^{-|\alpha|(x-\xi)}I_0[|\alpha|(x-\xi)]d\xi \tag{3.21}$$

$$=-\frac{1}{2m}\left\{F'(0)e^{-|\alpha|x}I_0(|\alpha|x)+\int_0^x F''(\xi)e^{-|\alpha|(x-\xi)}I_0[|\alpha|(x-\xi)]d\xi\right\} \tag{3.22}$$

In this case I_0 appears in place of K_0 and we are now in a position to calculate

$$J_n'=\int\xi^n e^{-|\alpha|(x-\xi)}I_0[|\alpha|(x-\xi)]d\xi. \tag{3.23}$$

The integral exsressions for the I-functions[14)] are as follows:

$$z^{-m}I_m(z)=z^{-m}I_{-m}(z)=\frac{1}{2^m\Gamma(m+1/2)\Gamma(1/2)}\int_{-1}^1 e^{-zt}(1-t^2)^{m-1/2}dt \tag{3.24}$$

$$\frac{d}{dz}[z^{-m}I_{-m}(z)]=\frac{1}{2^m\Gamma(m+1/2)\Gamma(1/2)}\int_{-1}^1 te^{-zt}(1-t^2)^{m-1/2}dt \tag{3.25}$$

where m is an integer. (This notation (m) is used only here, so that any confusion with the parameter m implying $\sqrt{M_\infty^2-1}$ does not occur.)

First,

$$J_0'=\int e^{-|\alpha|(x-\xi)}I_0[|\alpha|(x-\xi)]d\xi=\frac{1}{\pi}\int_{-1}^{1}(1-t^2)^{1/2}dt\int e^{-|\alpha|(x-\xi)-|\alpha|(x-\xi)t}d\xi \tag{3.26}$$

$$=\frac{1}{\pi}\int_{-1}^{1}(1-t^2)^{1/2}\frac{e^{-|\alpha|(x-\xi)(1+t)}}{|\alpha|(1+t)}dt$$

$$=\frac{1}{\pi|\alpha|}e^{-|\alpha|(x-\xi)}\left\{\int_{-1}^{1}e^{-|\alpha|(x-\xi)t}(1-t^2)^{-3/2}dt-\int_{-1}^{1}te^{-|\alpha|(x-\xi)t}(1-t^2)^{-3/2}dt\right\}$$

$$=-\frac{1}{|\alpha|}e^{-|\alpha|(x-\xi)}\left\{|\alpha|(x-\xi)I_1[|\alpha|(x-\xi)]+\frac{d}{d[|\alpha|(x-\xi)]}|\alpha|(x-\xi)I_1[|\alpha|(x-\xi)]\right\} \tag{3.27}$$

$$=-e^{-|\alpha|(x-\xi)}\{(x-\xi)I_1[|\alpha|(x-\xi)]+(x-\xi)I_0[|\alpha|(x-\xi)]\} \tag{3.28}$$

by use of the relation, $d/dz[zI_1(z)]=zI_0(z)$. Also integration of J_n's will be performed in a similar manner to the previous case.

For a circular-arc aerofoil we get from (3.22) and (3.28)

$$\varphi_x=\frac{4t}{m}e^{-|\alpha|x}\left\{\left(x-\frac{1}{2}\right)I_0(|\alpha|x)+xI_1(|\alpha|x)\right\}. \tag{3.29}$$

In the limit, $|\alpha|\to\infty$ and $m\to 0$ $(M_\infty=1+0)$, the above equation coincides with (3.16)

Differentiation of (3.29) gives

$$\varphi_{xx}=\frac{4t}{m}e^{-|\alpha|x}\left\{\left(\frac{|\alpha|}{2}+1\right)I_0(|\alpha|x)-\frac{|\alpha|}{2}I_1(|\alpha|x)\right\}. \tag{3.30}$$

The corresponding equation to (3.19) for the supersonic case in Maeder's theory is

$$\xi_\infty^{3/2}\frac{|\alpha|}{2}=e^{-|\alpha|/2}\left\{\left(\frac{|\alpha|}{2}+1\right)I_0\left(\frac{|\alpha|}{2}\right)-\frac{|\alpha|}{2}I_1\left(\frac{|\alpha|}{2}\right)\right\}. \tag{3.31}$$

From this we know that $|\alpha|/2$ has only a non-vanishing solution in this case.

§4. Sonic and Shock Points on the Aerofoil

The simultaneous equations (2.6) and (2.7) are rewritten in a much simplified form by introducing a new function,

$$f(x;\ \alpha)=\pm(\sqrt{|M_\infty^2-1|}/t)\varphi_x(x;\ K) \tag{4.1}$$

in which the double sign corresponds to $M_\infty\lesseqgtr 1$, as follows:

$$|\xi_\infty|^{3/2}=f(c^*;\ \alpha), \tag{4.2}$$

$$2\alpha|\xi_\infty|^{3/2}=f_x(c^*;\ \alpha). \tag{4.3}$$

Here c^* and α are unknown, ξ_∞ being a parmeter. In the present example, (3.17), (3.29) and (3.30) give immediately $f(x;\ \alpha)$ and $f_x(x;\ \alpha)$.

On the other hand, the position of the shock wave on the aerofoil should be determined by the other root c^{**} of the same equation (4.2) for a definite α and ξ_∞, according to the prescription given in the previous work.[1)]

Actual calculation of the above equations, however, is not easy because they include transcendental functions. In our case of a circular-arc aerofoil, several steps of the successive calculation were necessary with the use of Newton's method.*

In solving (4.2) and (4.3) in the present case, it is useful to know beforehand by investigating analytically the asymptotic behaviours of the equations that for $\alpha=0$, $c^*=1/2$ and ξ_∞

* The author had recourse to an electric computer of relay type at Yulin Denki Seiki Co. Ltd..

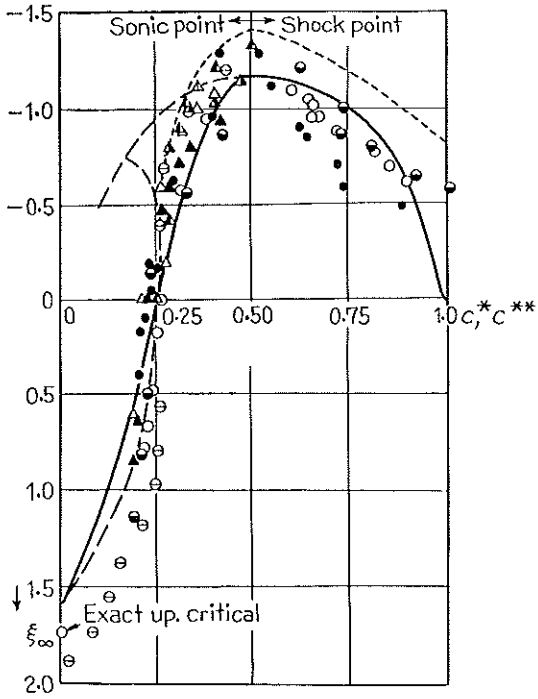

Fig. 1. Behaviours of the sonic and shock points on a circular-arc aerofoil.

Theory ------ Spreiter[6]
– – Maeder
—— Present

Experiment, Kawamura and Karashima[7]
● $t=0.106$ ○ $t=0.0808$
◒ $t=0.0544$ ⊖ $t=0.088$
Michel et al[3]
▲ $t=0.06$ ◭ $t=0.10$
△ $t=0.08$ ◮ $t=0.12$
Bryson[9]

$=-(4/\pi)^{2/3}$; for $\xi_\infty=0$, $\alpha=\pm\infty$ and $c^*=1/4$; and for $c^*=0$, $\alpha=-2$ and $\xi_\infty=2^{2/3}$. At the same time we have a knowlege by dealing with the equation of c^{**} that for $\alpha=0$ and $\xi_\infty=-(4/\pi)^{2/3}$, $c^{**}=1/2$; and for $\xi_\infty=0$ and $\alpha=\infty$, $c^{**}=1$. The calculated results are indicated in Table I as well as in Fig. 1.

In Fig. 1, the present result is compared with the theoretical ones by Maeder (linearized transonic flow theory) and by Spreiter (integral equation method)[6], and many experimental data.[7)-9] The sonic and shock points appear at first both on the midchord of a circular-arc aerofoil at the critical speed of the free stream, the former going ahead and the latter receding back monotonously with increasing Mach number. In this respect, Maeder's theory indicates a peculiar behaviour of the sonic point in the neighbourhood of the branch point, $\xi_\infty=-(2/\pi)^{2/3}$. The present result concerning the behaviour of the sonic point is in good accord with experiments throughout the whole transonic range of ξ_∞, though Spreiter's one is better for the smaller range of ξ_∞ near the critical speed. Furthermore the present method predicts the upper critical value of ξ_∞ very close to the exact one (=1.74, which can be found from the oblique-shock relation), whereas Spreiter's result by the local linearization method gives the value 2.08.[13]

Now with respect to the position of the shock wave on the aerofoil, it may be pointed out that the present theory predicts it much closer to the experimental data than Spreiter's although the experimental data show certain indefiniteness such that the shock wave

Table I. Solutions of (4.2) and (4.3).

c^*	α	$(-\xi_\infty)^{3/2}$	c^{**}	c^*	$\lvert\alpha\rvert$	$\xi_\infty^{3/2}$
0.500	0.000	1.2732(=4/π)	0.500	0.250	∞	0.0000
0.475	0.203	1.2468	0.575	0.225	11.300	0.1089
0.450	0.418	1.1838	0.645	0.200	6.480	0.3076
0.425	0.660	1.0908	0.711	0.175	4.807	0.5256
0.400	0.950	0.9697	0.772	0.150	3.900	0.7461
0.375	1.317	0.8227	0.825	0.125	3.325	0.9630
0.350	1.835	0.6500	0.872	0.100	2.912	1.1773
0.325	2.652	0.4594	0.910	0.075	2.605	1.3874
0.300	4.260	0.2648	0.941	0.050	2.360	1.5947
0.275	9.150	0.0970	0.967	0.025	2.165	1.7986
0.2625	19.100	0.0349	0.980			
0.250	∞	0.0000	1.000	0.000	2.000	2.0000

changes its position considerably depending on the thickness ratio of the aerofoil and the Reynolds number of the flow*; the shock wave predicted by Spreiter seem to recede too rapidly with increasing ξ_∞.

It is interesting to note that the nature of our curve which is nearly horizontal and flat at $x=0.5-0.75$ suggests unstableness of the position of the shock wave just after the lower critical value of ξ_∞ is surpassed. Namely if the main flow suffers non-uniformity expressed by ΔM_∞, the shock wave will be unstable and fluctuate from its original position by the amount

$$\Delta c^{**}=\frac{\partial c^{**}}{\partial \xi_\infty}\frac{2M_\infty{}^2+4}{3M_\infty\{(\gamma+1)M_\infty{}^2 t\}^{2/3}}\Delta M_\infty. \quad (4.4)$$

The thinner the aerofoil is, the more unstable is the position for the same grade of the assumed non-uniformity of the free stream.

§ 5. Pressure and Velocity Distributions

By use of the reduced velocity u and $f(x, \alpha)$, (2.3), (2.4) and (2.5) are simplified, as follows:

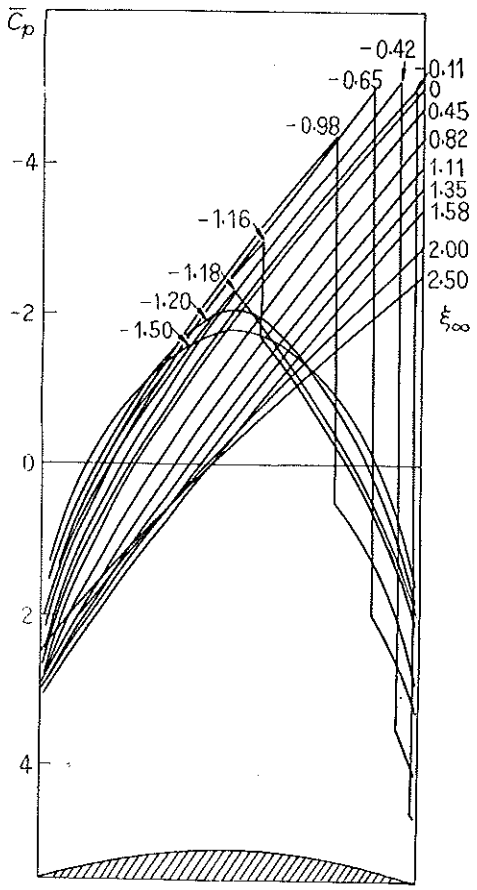

Fig. 2. Theoretical pressure distribution on a circular-arc aerofoil in terms of C_p, for various ξ_∞.

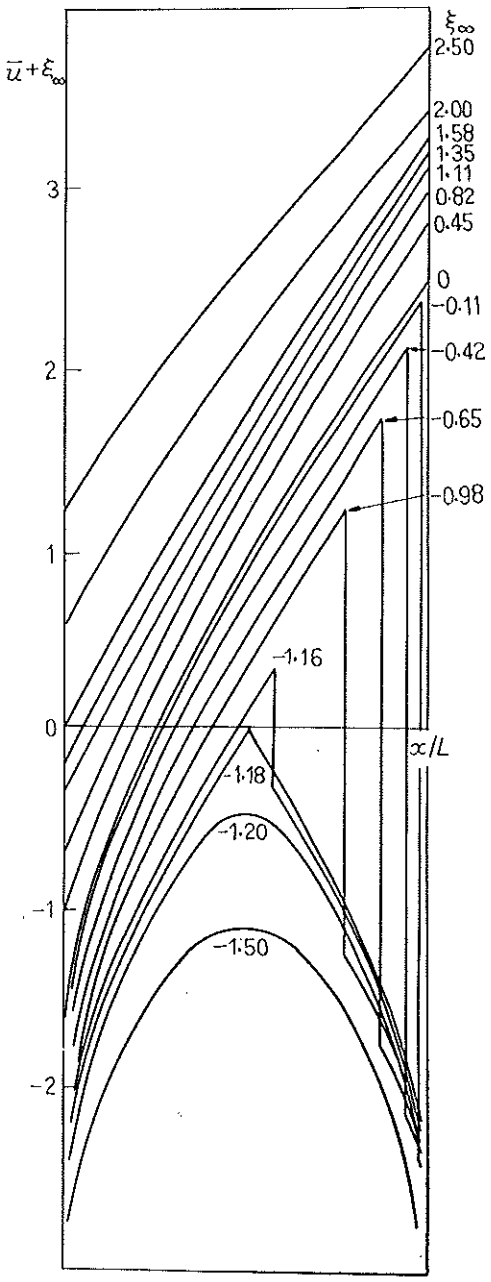

Fig. 3. Theoretical velocity distribution on a circular-arc aerofoil in terms of $u+\xi_\infty$, for various ξ_∞.

* In quoting the experiment of Ref. 7, the unpublished details of experimental data could be utilized thanks to kindness of the authors of Ref. 7.

$$u=\frac{\{M_\infty^2(\gamma+1)\}^{1/3}}{t^{2/3}}\Phi_x \tag{5.1}$$

$$=-\xi_\infty\pm\sqrt{\eta(x)} \tag{5.2}$$

$$\eta(x)=\xi_\infty^2+(1/|\xi_\infty|)f^2(c^*;\ \alpha)-2\sqrt{|\xi_\infty|}f(x;\ \alpha)+4\alpha\sqrt{|\xi_\infty|}\int_{c^*}^{x}f(x;\ \alpha)dx \tag{5.3}$$

the double sign corresponding to

$$\xi_\infty^2-\sqrt{|\xi_\infty|}f(x;\ \alpha)\leqq 0, \qquad \text{for} \quad M_\infty<1$$

and

$$\xi_\infty^2-\sqrt{|\xi_\infty|}f(x;\ \alpha)\geqq 0, \qquad \text{for} \quad M_\infty>1 \tag{5.4}$$

As α is uniquely related to ξ_∞, (5.2) is the expression consistent with the transonic similarity law.

By use of this expression, we obtain the two formulae for reduced physical quantities

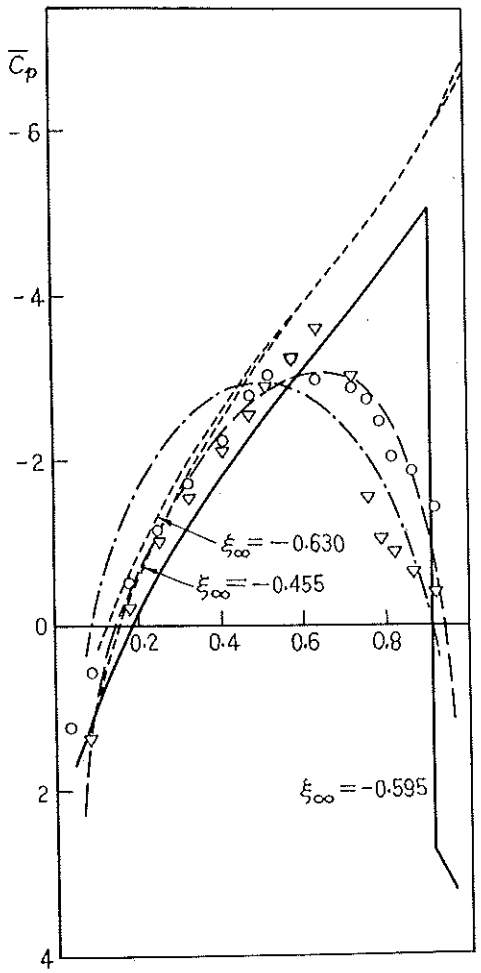

Fig. 4. Pressure distribution on a circular-arc aerofoil in the supercritical flow ($\xi_\infty\cong-0.526$).

Theory ------ Spreiter[12]
— — Maeder[11] ($\xi_\infty=-0.526$)
—— Present
—·— Prandtl-Glauert

Experiment, Liepmann[10]
○ $Re=8.77\times10^5$
△ $Re=1.75\times10^6$

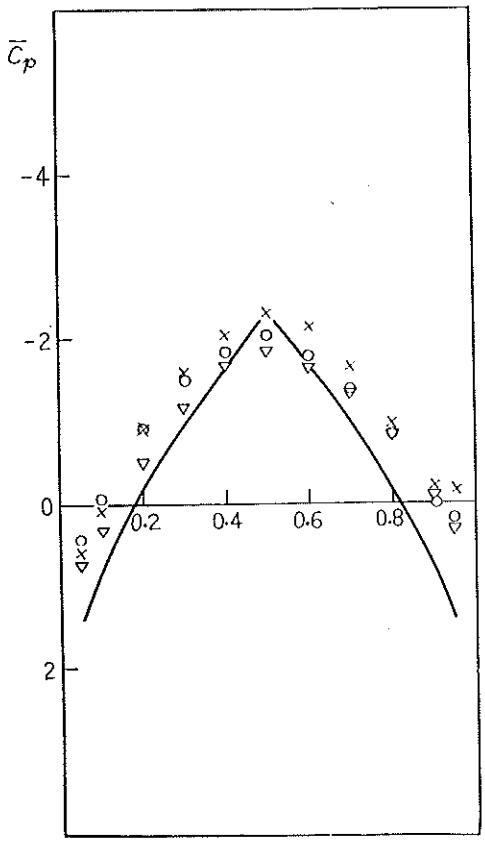

Fig. 5. Pressure distribution on a circular-arc aerofoil in the lower critical flow.

Theory —— Present ($\xi_\infty=-1.1745$)
Experiment, Michel et al[3]
○ $M_\infty=0.770$, $t=0.12$ ($\xi_\infty=-1.3226$)
× $M_\infty=0.835$, $t=0.08$ ($\xi_\infty=-1.1567$)
△ $M_\infty=0.870$, $t=0.06$ ($\xi_\infty=-1.0653$)

as follows;
for *pressure coefficient* C_p;

$$\overline{C}_p=\{M_\infty^2(\gamma+1)\}^{1/3}t^{-2/3}C_p=-2u \tag{5.5}$$

$$=2\xi_\infty\mp2\sqrt{\eta(x;\,\xi_\infty)} \tag{5.6}$$

for *local Mach mumber* M;

$$u+\xi_\infty^2=\{(\gamma+1)tM_\infty^2\}^{-2/3}\{(\gamma+1)M_\infty^2\Phi_x-(1-M_\infty^2)\}$$
$$=(M^2-1)/\{(\gamma+1)tM_\infty^2\}^{-2/3}\cong2(M-1)/\{(\gamma+1)t\}^{-2/3} \tag{5.8}$$

and we have only to remark that

$$u+\xi_\infty\gtrless0 \text{ corresponds to } M\gtrless1. \tag{5.8}$$

The both results calculated for various values of ξ_∞ are shown in Figs. 2 and 3. The

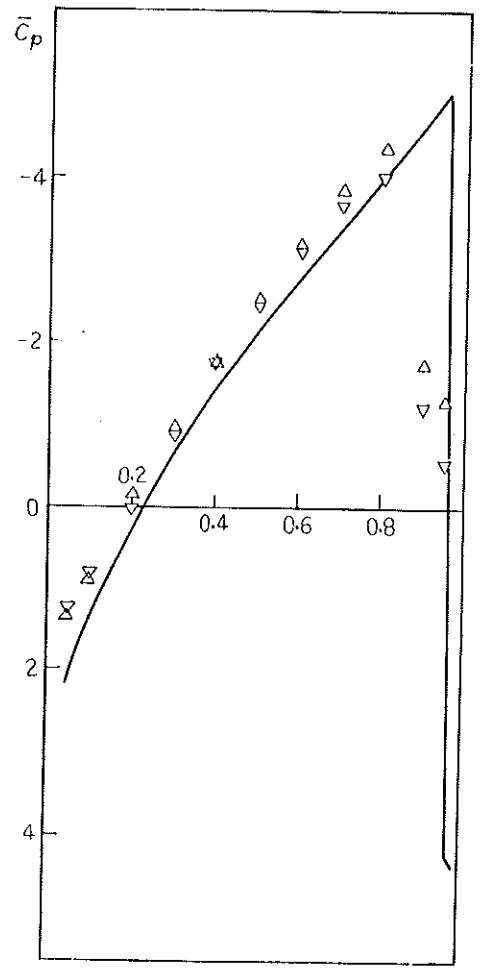

Fig. 6. Pressure distribution on a circular-arc aerfoil in the supercritical flow.
Theory —— Present ($\xi_\infty=-0.2110$)
Experiment, Michel et al[8]
△ $M_\infty=0.955$, $t=0.10$ ($\xi_\infty=-0.2422$)
▽ $M_\infty=0.970$, $t=0.06$ ($\xi_\infty=-0.2240$)

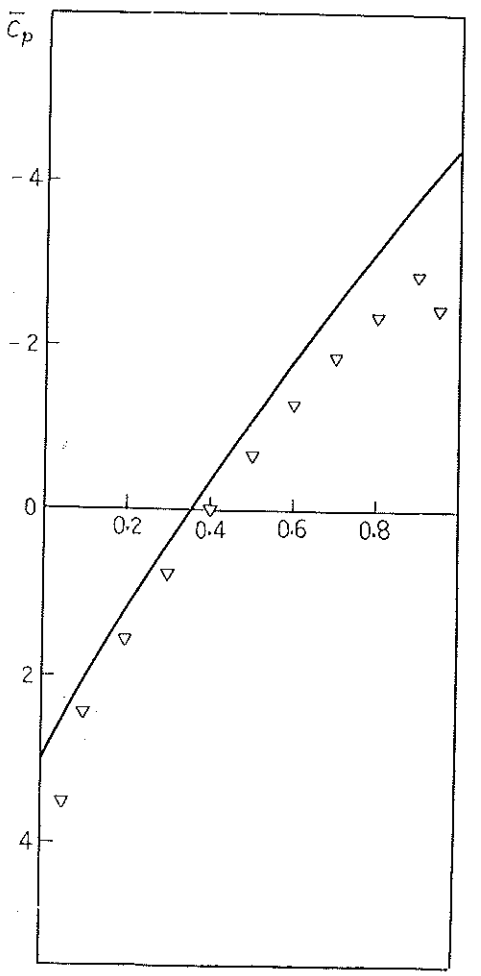

Fig. 7. Pressure distribution on a circular-arc aerofoil in the superonic, but below upper critical flow.
Theory —— Present ($\xi_\infty=0.8226$)
Experiment, Michel et al[8]
▽ $M_\infty=1.125$, $t=0.06$ ($\xi_\infty=0.8264$)

variations of them with ξ_∞ seem to be reasonable as a whole. In the sub- and supersonic extremities, they are in accord with the results obtained by the conventional linear theories. At the lower critical value of ξ_∞, the curve of the velocity distribution makes an angular shift at the sonic point and it is interesting to compare with the well-known critical state of pears on the aerofoil, and arrives at the trailing edge at $\xi_\infty=0$.

Fig. 4 is presented for comparison with other theories.[11),12)] They are compared with Liepmann's experiment[10)] which was performed for a circular-arc aerofoil of $t=0.12$ in the supercritical flow of $M_\infty=0.895$ ($\xi_\infty=-0.526$). First it is seen that Maeder's result[11)] is better in this régime of transonic flow (*cf.* Fig. 9), probably due to the viscous effect which destroys the formation of a shock wave near the aerofoil. Next, Spreiter's result[12)] overestimates the negative pressure on the aerofoil, particularly in the rear portion. This is in close relation to his prediction of rapid receding of the position of shock wave (described in the previous section). Thus, our prediction could be considered rather successful as a conclusion from the inviscid, nonlinear theory.

Figs. 5, 6 and 7 are provided in addition in order to compare our results with Michel's experiments (ONERA).[8)] They offer three typical examples of flows; that is, the lower critical, supercritical, and supersonic flows.

§6. Shock Wave at the Trailing Edge

We have learned that the normal shock arrives at the trailing edge when $\xi_\infty=0$. Then, what happens on the velocity discontinuity when ξ_∞ becomes positive? Certainly the velocity discontinuity will then lose the meaning of a normal shock and take the feature of an oblique shock, which we shall prove mathematically within the present theory as follows.

After the trailing edge, we should have

$$\varphi_x=\frac{1}{2m}\int_0^1 F'(\xi)\frac{\partial}{\partial\xi}e^{-|\alpha|(x-\xi)}I_0[|\alpha|(x-\xi)]d\xi \tag{6.1}$$

$$=-\frac{1}{2m}\left\{F'(0)e^{-|\alpha|x}I_0(|\alpha|x)-F'(1)e^{-|\alpha|(x-1)}I_0[|\alpha|(x-1)]\right.$$
$$\left.+\int_0^1 F''(\xi)e^{-|\alpha|(x-\xi)}I_0[|\alpha|x-\xi)]d\xi\right\} \tag{6.2}$$

$$=\frac{2t}{m}[e^{-|\alpha|x}\{(2x-1)I_0(|\alpha|x)+2xI_1(|\alpha|x)\}$$
$$-e^{-|\alpha|(x-1)}\{(2x-1)I_0[|\alpha|(x-1)]+2(x-1)I_1[|\alpha|(x-1)]\}] \tag{6.3}$$

with the aid of (3.28). In the limit when x approaches the trailing edge upstream, this becomes

$$\varphi_x(1+0)=\frac{2t}{m}[e^{-|\alpha|}\{I_0(|\alpha|)+2I_1(|\alpha|)\}-1]<0. \tag{6.4}$$

From (3.29), on the other hand, the limit when x approaches there downstream is obtained as

$$\varphi_x(1-0)=\frac{2t}{m}[e^{-|\alpha|}\{I_0(|\alpha|)+2I_1(|\alpha|)\}]>0. \tag{6.5}$$

Now from (6.4) and (6.5), the following relation can be derived;

$$Y(1-0)\geqq Y(1+0) \tag{6.6}$$

(Here it is noted that the last term of the right-hand side of (2.4) has the same value in both limits, since $\varphi(1\pm0)-\varphi(c^*)=\int_{c^*}^1\varphi_x dx$.)

The equality holds only when $M_\infty=1$ and at the extremity, $M_\infty\to\infty$. These results may be considered to elucidate qualitatively the above-mentioned fact, the resonable behaviour of the

supersonic flow at the trailing edge.

Moreover, it can be shown that when ξ_∞ is equal to 0.833 (which is smaller than the upper critical value), the oblique shock changes suddenly to that belonging to the weak family. The proof is as follows.

According to the rule (2.5), the sign to be attached to $\sqrt{Y(1+0)}$ should change from minus to plus when

$$\varphi_x(1+0)=(1-M_\infty^2)/[(\gamma+1)M_\infty^2]. \tag{6.7}$$

This condition is expressed by use of (6.4) as

$$2[e^{-|\alpha|}\{I_0(|\alpha|)+2I_1(|\alpha|)\}-1]=-\xi_\infty^{3/2} \tag{6.8}$$

Since $|\alpha|$ is already uniquely related to ξ_∞ as described in § 4., we can solve (6.8) and obtain $|\alpha|\doteqdot 3.85$ and $\xi_\infty^{3/2}\doteqdot 0.76$ ($\xi_s\doteqdot 0.833$). Then we have

$$Y(1+0)=2K/[(\gamma+1)M_\infty^2]\cdot\{\varphi(1+0)-\varphi(c^*)\}>0. \tag{6.9}$$

For example, velocity distributions for two cases are shown in Fig. 8; each corresponds to ξ_∞, a little smaller (a), and larger (b) than this value, respectively.

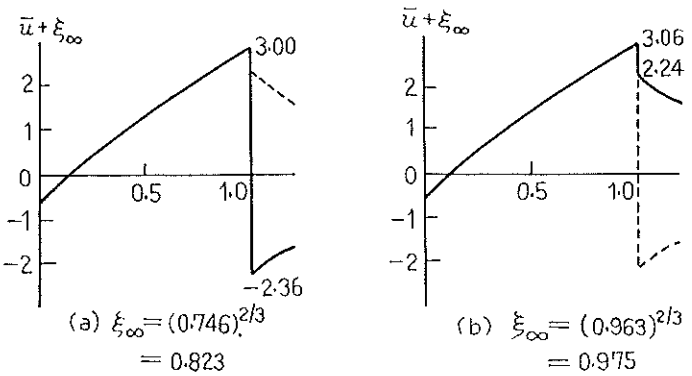

Fig. 8. Illustration of conversion of the shock-wave family at the trailing edge of a circular-arc aerofoil. ($\xi_\infty=0.833$ is the point of conversion)

This result is qualitatively correct. Because, first, when the supersonic flow is deflected by a very small angle at the trailing edge, it can either drop to subsonic through a strong shock wave, or remain supersonic through a weak shock wave, as is known from the consideration by the shock polar; next there is a normal shock at the trailing edge in the case of $M_\infty=1$ in the present theory and, on the other hand, naturally we have a weak shock for higher Mach numbers where the flow about there is purely supersonic; and therefore it is quite unavoidable that a sudden, discontinuous change of the family of shock occurs at some value of M_∞ larger than one with increasing Mach number. As is proved already ((6.6)), the weak shock tends to the Mach wave in the supersonic linear theory.

§ 7. Pressure Drag

The reduced drag coefficient $\bar{C}_d$ is evaluated as follows:

$$\bar{C}_d=\frac{\{(\gamma+1)M_\infty^2\}^{1/3}}{t^{5/3}}C_d=\frac{\{(\gamma+1)M_\infty^2\}^{1/3}}{t^{5/3}}\int_0^1 F'(x)C_p(x)dx \tag{7.1}$$

$$=\int_0^1(1/t)F'(x)\bar{C}_p(x;\xi_\infty)dx. \tag{7.2}$$

In case of a circular-arc aerofoil,

$$\bar{C}_d = \int_0^1 4(1-2x)\bar{C}_p(x;\xi_\infty)dx. \tag{7.3}$$

For the case of $M_\infty<1$, the range of integration is conveniently reduced to (0.05—0.95), because the flow has singularities of the same type at the leading and trailing edges, and the maximum error of $\bar{C}_d$ due to this approximation will be within about 0.1.

The calculated results are shown in Fig. 9 with other data. It is noted, however, that in our result a slightly negative drag which amounts to -2.0 at most is obtained within a very small range of ξ_∞ just above the lower critical value. It is probably due to the concentrated effect of the theoretical error in the neighbourhood of the leading and trailing edges;[1] but it may be considered practically insignificant.

Comparing with the experimental data in the figure, Maeder's theory seems to give a good result at least for ξ_∞ near zero, in the subsonic side but it fails for other ranges of ξ_∞.[11] One of his results that there exists a supercritical, symmetric, shock-free solution for ξ_∞ smaller than $-(2/\pi)^{2/3}$ contradicts the experimental fact. On the other hand, Spreiter's integral equation method[6),12)] results in the unnatural, too rapid increase of drag for ξ_∞ just above the lower critical value, though it predicts that critical value itself rather well. This

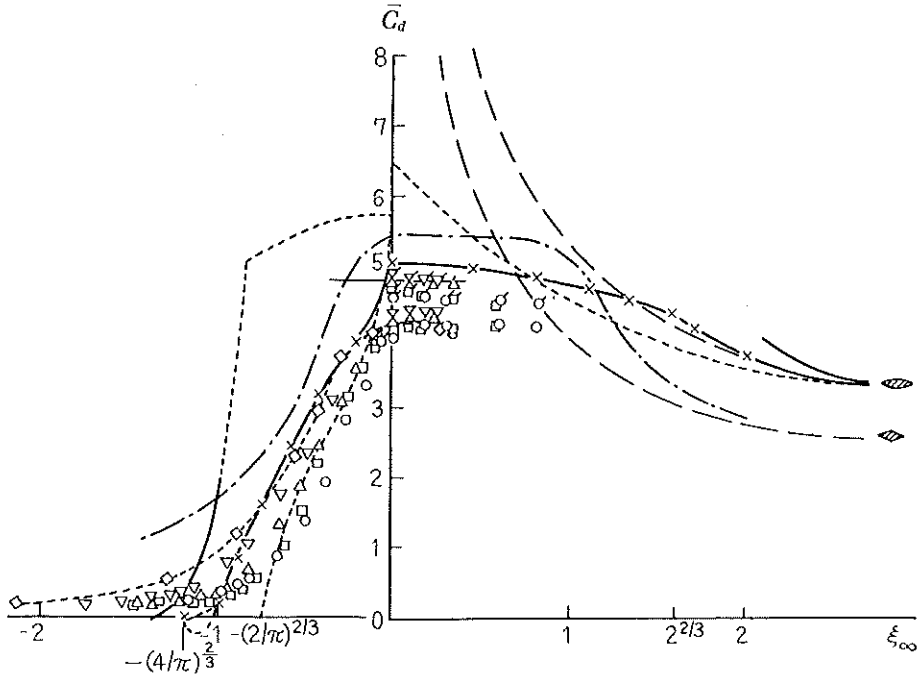

Fig. 9. Reduced pressure drag coefficient $\bar{C}_d$ of a circular-arc aerofoil versus ξ_∞.

Theory
- Spreiter (Integral Eq.)[12)]
- Spreiter (Local Linearization)[6),13)]
- Maeder[11)]
- × Present
- Linear Theory
- Diamond Aerofoil

Experiment, Michel et al[8)]
- ○ $t=0.06$
- □ $t=0.08$
- △ $t=0.10$
- ▽ $t=0.12$

Extrapolated Drag

(These data have been cited from Speriter's work[18)].)

Maeder[11)]
- ◇ $t=0.1$ (slotted wall)

is considered a reflection of the rapid receding of the shock wave and the overestimation of the velocity distribution in his result as were stated before. The local linearization method gives good results locally for the proper ranges of ξ_∞.[6),13)] But it seems that the phenomenon of sonic freezing is not so remarkable in the subsonic side as expected, in this theory from the experimental point of view. Thus among all these results, the present theory seems to be the most satisfactory as a whole, considering the general trend of experiments.

For reference, the famous drag-curve for a diamond aerofoil is added, which was given theoretically by Trilling, Guderley and Yoshihara, and Vincenti and Wagoner. The both bear a much qualitative resemblance but that the lower critical value of ξ_∞ for a diamond aerofoil vanishes whereas that for the present aerofoil is equal to $-(4/\pi)^{2/3}$.

§8. Concluding Remarks

As an example of application of the author's method in the previous paper, various transonic flows around a circular-arc aerofoil were calculated with success. This method can be directly applied to any thin aerofoil as far as its profile is expressed by a polynomial. If a high speed computer is available, applicability will further be enlarged.

These results are significant in verifying the following facts: First, transonic flows around a thin aerofoil can be treated by systematical analysis throughout the whole range of Mach number so that a plausible transition of the flows with M_∞ be given in the first-order approximation, and secondly the quadratic nature of the nonlinear equation gives rise to the shock wave in the flow field inevitably in some case. This is also consistent with the general view that it is probably impossible to have a smooth supersonic zone enclosed within a subsonic field.

Finally the author wishes to express his hearty thanks to members of the National Aeronautical Laboratory for their valuable discussions.

References

1) I. Hosokawa: J. Phys. Soc. Japan **15** (1960) 149.
2) K. Oswatitsch and F. Keune: Proc. Conf. on High Speed Aeronautics, Polytech. Inst. Brooklyn (1955) 113.
3) P. F. Maeder and H. U. Thommen: J. Aero. Sci. **23** (1956) 187.
4) I. Hosokawa: J. Phys. Soc. Japan **15** (1960) 2080.
5) C. C. Lin and S. I. Rubinov: J. Math. Phys. **27** (1948) 105.
6) J. R. Spreiter, A. Y. Alksne and B. J. Heytt: NACA Tech. Note 4148 (1958)
7) R. Kawamura and K. Karashima: Aero. Research Inst. Univ. Tokyo Rep. no. 342 (1959).
8) R. Michel, F. Marchaud and J. Le Gallo: ONERA, Publication no. 65 (1953).
9) A. E. Bryson: NACA Tech. Rep. 1094 (1952).
10) H. W. Liepmann: J. Aero. Sci. **13** (1946) 623.
11) P. F. Maeder: Proc. 9th Intern. Congr. Appl. Mech., vol. 2 (1957) 15.
12) J. R. Spreiter and A. Y. Alksne: NACA Tech. Rep. 1217 (1955) 31.
13) J. R. Spreiter and A. Y. Alksne: NACA Tech. Note 3970 (1957) 50.
14) G. N. Watson: *Theory of Bessel Functions.* (Cambridge, 1922) 171 p.

Nomenclatures

x, y, z = Cartesian coordinates; as subscripts, derivatives with respect to coordinates.
U_∞, M_∞ = Velocity and Mach number, respectively, of the free stream parallel to the x-axis.
γ = Ratio of specific heats.
Φ = Perturbation velocity potential devided by U_∞.
φ = Linearized potential due to Oswatitsch and Maeder.
K = Constant due to linearization of the transonic flow equation.
g = Nonlinear correction term to φ.
τ = Parameter of small disturbance in the transonic flow.
t = Thickness ratio.
c^* = Location of the sonic point on the body.
c^{**} = Location of the shock point on the body.
Y = Discriminant of the root for g_x.
F = Distribution of the cross-sectional area of the body whose length is assumed unity.
s = Shape function of the body in the meridian plane.
α = $K/2\beta^2$ or $-K/2m^2$
β^2 = $-m^2=1-M_\infty^2$
K_0, I_0 = Modified Bessel functions of the zeroth order.
f_0, ω = Amplitude and angular frequency, respectively, of a sinusoidal wall.
N = $|\beta|/(2f_0).\varphi_x$
C_p = $-2\varphi_x$ = pressure coefficient
$\bar{C}_p$ = $-2\bar{u}=-2\dfrac{[(\gamma+1)M_\infty^2]^{1/3}}{t^{2/3}}\varphi_x$ = reduced pressure coefficient.
ξ_∞ = $(M_\infty^2-1)/[(\gamma+1)M_\infty^2 t]^{2/3}$ = transonic similarity parameter.
C_d = drag coefficient.
$\bar{C}_d$ = $\dfrac{[(\gamma+1)M_\infty^2]^{1/3}}{t^{5/3}}$ = reduced drag coefficient.

NAL TR-9T

NATIONAL AERONAUTICAL LABORATORY

Studies on the Small Disturbance Theory of Transonic Flow (I)
—Nonlinear Correction Theory—

July, 1962 p. 29

In order to approach to the flow near thin wings and bodies flying at transonic speed, the small disturbance theory of transonic flow theory is studied from a new point of view. First, the mathematical ground of the linearized transonic flow theory originating with Oswatisch is investigated by introduction of the correction term for complementing the linearized flow field, and therefrom a more exact and reasonable method of approximation is developed. Two examples of approximation of the method are given; about the flows past a wavy wall and on a circular-arc aerofoil with various free stream Mach numbers. As a result, it turns out that the present theory can reveal many plausible general features of transonic flows.

I. Iwao Hosokawa
II. NAL TR-9T
III. 533.6.011.35
: 517.93

NAL TR-9T

NATIONAL AERONAUTICAL LABORATORY

Studies on the Small Disturbance Theory of Transonic Flow (I)
—Nonliner Correction Theory—

July, 1962 p. 29

In order to approach to the flow near thin wings and bodies flying at transonic speed, the small disturbance theory of transonic flow theory is studied from a new point of view. First, the mathamatical ground of the linearized transonic flow theory originating with Oswatitsch is investigated by introduction of the correction term for complementing the linearized flow field, and therefrom a more exact and reasonable method of approximation is developed. Two examples of approximation of the method are given; about the flows past a wavy wall and on a circular-arc aerofoil with various free stream Mach numbers. As a result, it turns out that the present theory can reveal many plausible general features of transonic flows.

I. Iwao Hosokawa
II. NAL TR-9T
III. 533.6.011.35
: 517.93

NAL TR-9T

NATIONAL AERONAUTICAL LABORATORY

Studies on the Small Disturbance Theory of Transonic Flow (I)
—Nonlinear Correction Theory—

July, 1962 p. 29

In order to approach to the flow near thin wings and bodies flying at transonic speed, the small disturbance theory of transonic flow theory is studied from a new point of view. First, the mathematical ground of the linearized transonic flow theory orginating with Oswatitsch is investigated by introduction of the correction term for complementing the linearized flow field, and therefrom a more exact and reasonable method of approximation is developed. Two examples of approximation of the method are given; about the flows past a wavy wall and on a circular-are aerofoil with various free stream Mach numbers. As a result, it turns out that the present theory can reveal many plausible general features of transonic flows.

I. Iwao Hosokawa
II. NAL TR-9T
III. 533.6.011.35
: 517.93

NAL TR-9T

NATIONAL AERONAUTICAL LABORATORY

Studies on the Small Disturbance Theory of Transonic Flow (I)
—Nonlinear Correction Theory—

July, 1962 p. 29

In order to approach to the flow near thin wings and bodies flying at transonic speed, the small disturbance theory of transonic flow theory is studied from a new point of view. First, the mathematical ground of the linearized transonic flow theory originating with Oswatitsch is investigated by introduction of the correction term for complementing the linearized flow field, and therefrom a more exact and reasonable method of approximation is developed. Two examples of approximation of the method are givn; about the flows past a wavy wall and on a circular-are aerofoil with various free stream Mach numbers. As a result, it turns out that the present theory can reveal many plausible general features of transonic flows.

I. Iwao Hosokawa
II. NAL TR-9T
III. 533.6.011.35
: 517.93

TECHNICAL REPORT OF NATIONAL
AERONAUTICAL LABORATORY
TR-9T

航空技術研究所報告9号(欧文)

昭和37年7月 発行

発行所 航空技術研究所
東京都三鷹市新川700
電話武蔵野(0422)(3)5171(代表)

印刷所 笠井出版印刷社
東京都港区芝南佐久間町1の53

Published by
NATIONAL AERONAUTICAL LABORATORY
700, Shinkawa, Mitaka, Tokyo
JAPAN

ERRATA

Errata in Hosokawa : Studies on the Small Disturbance Theory of Transonic Flow (I)

正　誤　表

表誌　TECHNICAL

Page	Line	Now Reads	Should Read
0	15	view point	viewpoint
1	3	Oswaititsch	Oswatitsch
1	18	Speriter's	Spreiter's
1	28	giving	give
2	9	quatities	quantities
5	33(5.1)	$\varphi(x,\ r)\cdots(-1^n)$	$\varphi(x,\ y)\cdots(-1)^n$
6	42(5.4)	$0\leqq\alpha\leqq 1$	$0\leqq x\leqq 1$
6	Footnote, 5	becaus	because
7	32(A6)	$F'(x)$	$F'(\xi)$
7	36(A8)	$\sum_{n=0}$	$\sum_{n=0}$
7	Footnote, 1	form	from
8	2(A 9)	$\sum_{k=0}^{n}$	$\sum_{k=0}^{n}$
8	7(A11)	$\varphi(x,\ r)$	$\varphi(x,\ y)$
8	9(A12)	$\dfrac{\exp[-Kr^2/4(x-\xi)]}{x-\xi}$	$\dfrac{\exp[-Kr^2/4(x-\xi)]}{x-\xi}d\xi$
8	19(A16)	J^1	J_1
11	36(4.10)	$\xi_\infty\leqq-\pi^{2\ 2}$	$\xi_\infty\leqq-\pi^{2.3}$
12	Fig. 2	$\Delta C_p/2$	$\Delta\bar{C}_p/2$
13	3(4.15)	$\lvert\xi\rvert^{3/2}$	$\lvert\xi_\infty\rvert^{3/2}$
13	7(4.17)	$\lvert\xi\rvert^{3\ 2}$	$\lvert\xi_\infty\rvert^{3/2}$
13	Fig. 3	terms of C_p	terms of $\bar{C}_p$
14	19(4.26)	$\Delta C_p\ /2$	$\Delta\bar{C}_p/2$
17	6(2.5)	$\lesssim$	$\gtrsim$
17	16~17	take the~solution from	take the fixed value of the (lower or upper) critical point in order to ensure the continuity of the solution from

Page	Line	Now Reads	Should Read
17	32(3.1)	ξd	$d\xi$
17	33(3.2)	$\int_0^{x-my}$	$\int_0^{x-m\|y\|}$
18	18	$e^{x(x-\xi)(1\mp t)}$	$e^{\alpha(x-\xi)(1\mp t)}$
18	21	$x \lesseqgtr \xi$	$x \gtreqless \xi$
20	4(3.26)	$e^{-\|\alpha\|(x\sim\xi)\sim\|\alpha\|(x-\xi)t}$	$e^{-\|\alpha\|(x-\xi)-\|\alpha\|(x-\xi)t}$
20	5	$(1-t^2)^{1/2}$	$(1-t^2)^{-1/2}$
20	18	$\|x\|/2$	$\|\alpha\|/2$
20	26	parmeter$\cdots$,(3.17),$\cdots$,	parameter$\cdots$,(3.15),(3.17),$\cdots$
21	3	knowlege	knowledge
21	16	monotonously	monotonically
21	Fig. 1	$\ominus$ $i=0.088$ Bryson[9]	Bryson[9] $\ominus$ $t=0.088$
22	15	u	$\bar{u}$
22	Fig. 2	of C_p	of $\bar{C}_p$
22	Fig. 3	of $u+\xi_\infty$	of $\bar{u}+\xi_\infty$
23	1(5.1)	u	$\bar{u}$
24	3(5.5)	u	$\bar{u}$
24	5	mumber	number
24	6	$u+\xi_\infty{}^2$	$\bar{u}+\xi_\infty$
24	9(5.8)	u	$\bar{u}$
25	5	of pears on	of the one-dimensional flow. For ξ_∞ above the lower critical value, a normal shock wave appears on
25	26(6.2)	$\|\alpha\|x-\xi)$	$\|\alpha\|(x-\xi)$
26	11	ξ_8	ξ_∞
27	title	Non-tlifting	Non-lifting
27	6	-2.0	-0.2
27	11	zero,$\cdots$side but	zero$\cdots$side, but
27	Fig. 9	Spreiter's work[13]	Spreiter's work[13]
28	4	expected,$\cdots$theory from	expected$\cdots$theory, from
29	21	φ_x	Φ_x
29	22	φ_x	Φ_x
29	25	$\frac{[(\gamma+1)M_\infty{}^2]^{1/3}}{t^{5/3}}$ —— =	$\frac{[(\gamma+1)M_\infty{}^2]^{1/3}}{t^{5/3}} C_d =$